Theory of collision effects in Doppler-free spectroscopy*

Paul R. Berman
Physics Department, New York University, 4 Washington Place, New York, New York 10003
(Received 1 December 1975)

A theory of the influence of binary collisions on the line shapes associated with Doppler-free spectroscopy is presented. The specific calculation is for two-photon absorption through a real or virtual intermediate state, but the extension of the results to alternative level schemes is included. Collisions are treated quite generally at first, but, ultimately, a simple but reasonable collision model is adopted to properly account for both the "phase-interrupting" and "velocity-changing" aspects of collisions. It is shown that collisional processes can be used to distinguish between the "two-quantum" and "stepwise" contributions to the two-photon excitation rate. Moreover, it is demonstrated that systematic experimental line-shape investigations, in addition to providing tests of current collision theories, can lead to values for collision broadening and shift parameters, excitation transfer rates, magnetic substate relaxation rates, velocity-changing collision rates, and collision kernels. Consequently, Doppler-free spectroscopy can provide a new and important probe of collision effects in atomic and molecular systems.

I. INTRODUCTION

While most of the initial interest in the use of laser spectroscopy has centered on the achievement of ultrahigh-resolution spectra, there have been some attempts to use lasers as a probe of collisional processes occurring within atomic and molecular systems. Narrow-band tunable laser sources can provide the means for obtaining both qualitative and quantitative data on collisions involving either excited or ground-state atoms. One class of experiments exploiting the high power and monochromaticity of lasers is atom-atom or electron-atom scattering in which the target atoms have been selectively excited by a laser.[1] Such experiments will provide excited-state differential-scattering cross sections which have been, for the most part, previously unobtainable. This paper is concerned with the theory of another class of experiments whose aim it is to provide new information on collisional relaxation mechanisms in atomic and molecular systems.

The relaxation parameters we have in mind are those which manifest themselves in the line shapes associated with atomic and molecular systems. Among these parameters, one might list broadening and shift coefficients, collisional quenching rates, rates for collisional relaxation of magnetic substates, velocity thermalization rates, and collision kernels. The determination of these parameters is important not only for the proper interpretation of experiments where collisions play a role, but also for providing some clues as to the nature of the interatomic potential giving rise to the relaxation. In particular, laser saturation spectroscopic techniques permit the elimination of the broad Doppler background encountered in standard spectroscopy, enabling one to have a more sensitive measure of the manner in which collisions perturb the energy levels and alter the velocity of the active (emitting or absorbing) atoms.

Only recently have theories appeared which purport to properly account for both the "velocity-changing" and "energy-level perturbation" aspects of collisions.[2-4] As will be described in this work, laser spectroscopy can be used to test the predictions of these theories. The standard type of experiment[5-12] involves exciting an atomic transition with a nearly monochromatic source and then probing either the same or a coupled transition with another laser source. To be specific, we shall consider the upward cascade shown in Fig. 1. If the lasers propagate in opposite directions, this scheme corresponds to the case of resonant enhanced two-photon spectroscopy recently discussed by Liao and Bjorkholm.[13]

To get some qualitative idea of the role of collisions, imagine that the lasers are polarized in a manner which would render it impossible to populate the upper level in the absence of collisions. The only way that upper-level population could be attained is for collisions to reorient the magnetic sublevel population of the intermediate state. Thus the upper-state population serves to monitor magnetic relaxation processes. Moreover, by varying the laser frequency driving the 2-3 transition and monitoring the upper-state population, one can gain information on any velocity changes incurred by the atom when the collision reoriented the magnetic sublevels.

It is the purpose of this paper to provide both a formal analysis of the collisional problem outlined above and a specific calculation for a simple but reasonable collision model. A few other calculations have appeared,[14-17] but the collision mod-

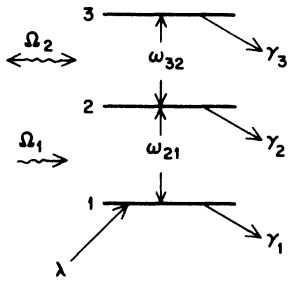

FIG. 1. Energy-level scheme considered in this work. Levels 1, 2, and 3 may each contain a number of degenerate sublevels.

els used and the connection of those models with the rigorous theories has not been clearly indicated. In Sec. II the physical system under consideration and approximations of the theory will be discussed. In Sec. III, a calculation of the upper-state population (Fig. 1) in the absence of collisions is made for weak laser fields of arbitrary polarization. The distinction between two-quantum and stepwise excitation is mentioned.[11,18,19] Collisions are incorporated into the calculation in Sec. IV and the nature of the solution is discussed in Sec. V. Specific results for a $J=0\rightarrow 1\rightarrow 0$ cascade is given in Sec. VI. Comments on generalizing the results to other level schemes are presented in Sec. VII and the available experimental results are discussed in Sec. VIII. Section IX contains a summary of the paper.

It might be well worth noting that some qualitative feel for the role of collisions may be obtained by referring to the line shapes depicted in Figs. 2–5. The mathematical detail leading to line shapes is given in Secs. II–VI.

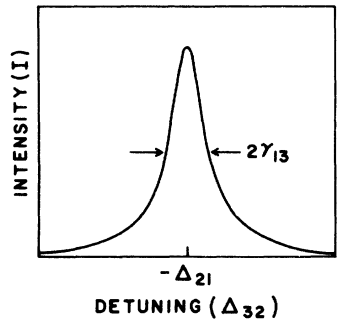

FIG. 2. Two-photon excitation line shape [Eq. (29)] in the absence of collisions. The line is a Lorentzian centered at $\Delta_{32}=-\Delta_{21}$, with HWHM of γ_{13}.

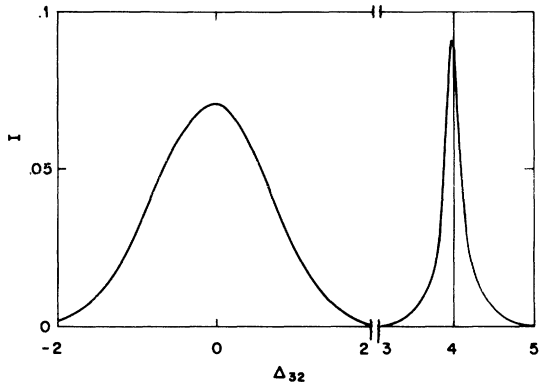

FIG. 3. Line shape [Eq. (49)] for a detuning $\Delta_{21}=-4.0ku$, when collisions are present and levels 1, 2 and 3 are nondegenerate. Values of the detuning Δ_{32} are in units of ku, and the intensity I is in the dimensionless units chosen such that the corresponding no-collision line shape would have a maximum intensity of unity. The vertical line indicates the central position of the no-collision line shape which would have a HWHM of 0.01 on this scale. For values of the collision parameters, see the text.

II. PHYSICAL SYSTEM AND APPROXIMATIONS

The physical system consists of active atoms which interact with radiation fields and undergo collisions with perturber atoms. The active-atom

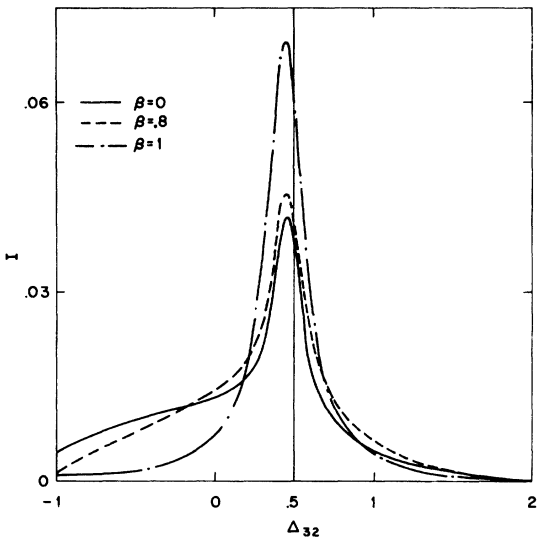

FIG. 4. Line shape [Eq. (54)] for a detuning $\Delta_{21}=-0.5ku$, no degeneracy in levels 1, 2, or 3, and three values of the collision-strength parameter β ($\beta=0$—strong collisions, $\beta=0.8$—moderate collisions, $\beta=1$—weak collisions). The collision parameters are the same as those used in Fig. 3 and the value of $\alpha=\gamma_2/[\gamma_2+\Gamma(2)]$ is chosen equal to $\frac{1}{3}$.

energy-level scheme is shown in Fig. 1. Levels 1 and 3 have the same parity, which is opposite that of level 2. Level 1 is pumped at some rate λ and each of the levels (1, 2, 3) decays with rates given by the corresponding phenomenological damping constants $\gamma_1, \gamma_2, \gamma_3$. The important situation of level 1 representing the ground state may be taken as a limiting case of the above scheme in which $\lambda \to 0$, $\gamma_1 \to 0$, but the ratio λ/γ_1 remains finite. While each of the levels may themselves consist of a number of degenerate states, the energy intervals $\hbar\omega_{21}$ between levels 2 and 1 and $\hbar\omega_{32}$ between levels 3 and 2 are assumed to be much greater than the thermal energy. Consequently, collisions may cause transitions among the degenerate substates *within* any of the levels but cannot induce transitions between states 1, 2, and 3.

The system is subjected to two fields,

$$\vec{E}_1(\vec{R}, t) = \mathrm{Re}[\vec{\mathcal{E}}_1 \exp i(\vec{k}_1 \cdot \vec{R} - \Omega_1 t)] \ , \tag{1a}$$

$$\vec{E}_2(\vec{R}, t) = \mathrm{Re}[\vec{\mathcal{E}}_2 \exp i(\vec{k}_2 \cdot \vec{R} - \Omega_2 t)] \ , \tag{1b}$$

where $\vec{k}_1$ and $\vec{k}_2$ are the propagation vectors, Ω_1 and Ω_2 the frequencies, and $\vec{\mathcal{E}}_1$ and $\vec{\mathcal{E}}_2$ the complex amplitudes of fields $\vec{E}_1$ and $\vec{E}_2$, respectively. The presence of the fields leads to a population of level 3 which is then monitored in some appropriate manner (i.e., by a measure of the fluorescence from level 3). Thus experimentally one may determine the population of level 3 as a function of Ω_1 and Ω_2, either of which may be varied.

The frequencies ω_{21}, ω_{32}, Ω_1, and Ω_2 are taken to satisfy the following inequalities:

$$|\omega_{21} - \omega_{32}| \gg k_1 u \text{ or } k_2 u \ , \tag{2a}$$

$$|\Omega_1 - \omega_{21}| \ll |\Omega_2 - \omega_{21}| ; \quad |\Omega_2 - \omega_{32}| \ll |\Omega_1 - \omega_{32}| , \tag{2b}$$

where u is the most probable speed of the active atoms. Equation (2a) ensures that any one field cannot be resonant with both transitions $1 \leftrightarrow 2$ and $2 \leftrightarrow 3$, while (2b) implies that field $\vec{E}_1$ effectively drives only the $1 \leftrightarrow 2$ transition and $\vec{E}_2$ effectively drives only the $2 \leftrightarrow 3$ transition. Furthermore, we shall assume that fields $\vec{E}_1$ and $\vec{E}_2$ are weak enough so that perturbation theory is applicable.

For simplicity, the perturber pressure is assumed low enough ($\lesssim 100$ Torr) such that only binary collisions need be considered and any resonant excitation exchange between active atom and perturber is neglected (i.e., only foreign-gas collisions are treated). In addition, the duration of a collision $\tau_c \simeq 10^{-12}$ sec is taken to be effectively instantaneous relative to other relevant time scales in the problem (impact approximation). This assumption requires that the frequencies Ω_1 and Ω_2 satisfy

$$|\Omega_1 - \omega_{21}|\tau_c \ll 1 \quad \text{and} \quad |\Omega_2 - \omega_{32}|\tau_c \ll 1 \ .$$

Finally, we neglect any radiation trapping which could also serve as a magnetic substate relaxation mechanism.

With the assumptions given above, general excitation line-shape formulas will be derived. Appropriate generalizations of the theory to remove some of the above restrictions will be given in Sec. VII. Actual illustrations of theoretical line shapes will be given for a specific case of current interest—two-photon Doppler-free excitation[12,13] from an atomic ground state. The Doppler-free condition is achieved by finding a level scheme which may be excited by counterpropagating fields of nearly equal frequency, $\vec{k}_1 \approx -\vec{k}_2$, such that

$$|(\vec{k}_1 + \vec{k}_2) \cdot \vec{v}| \ll \gamma_3 \ . \tag{3}$$

[The term Doppler-free refers to the cancellation of Doppler shifts that occurs in two-quantum processes with counterpropagating waves, provided Eq. (3) is satisfied.] Recalling that Eqs. (2) require the field frequencies to be significantly *different*, so that each field drives only one transition, one can combine Eqs. (2) and (3) to obtain the overall condition

$$\gamma_3/k_1 u > u/c \ ,$$

which must be satisfied for resonantly enhanced Doppler-free excitation. If condition (3) is not

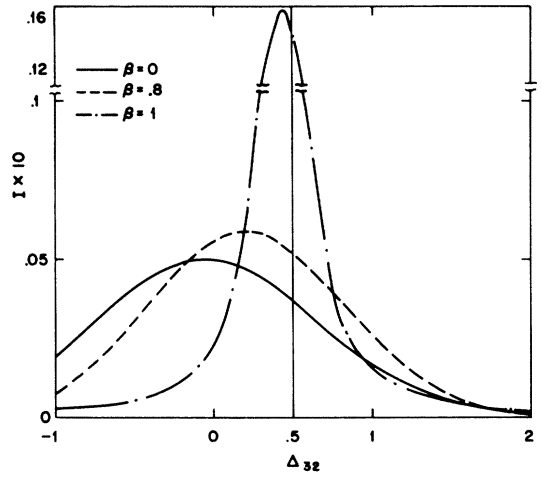

FIG. 5. Line shape [Eq. (6)] when levels 1, 2, and 3 have J values of 0, 1, and 0, respectively. The applied field $\vec{E}_1$ is LCP with propagation vector $\vec{k}_1$, and field $\vec{E}_2$ is RCP with propagation vector $\vec{k}_2 = -\vec{k}_1$. The detuning ($\Delta_{21} = -0.5ku$) and collision parameters are the same as those used in Fig. 4.

appropriate to the given experimental situation, the more general line-shape formulas must be used. The relevant equations for such cases are given in Appendix B.

It is somewhat misleading to refer to Eq. (3) as a requirement for two-photon Doppler-free spectroscopy, since narrow Doppler-free resonances may be obtained even if Eq. (3) is not valid. Such techniques are commonly used in saturation spectroscopy when frequencies Ω_1 and Ω_2 are chosen to lie within the Doppler width of transitions $1-2$ and $2-3$, respectively. In that case, only a small velocity subset of atoms contributes to line-shape formation and the resultant linewidth is on the order of the natural widths of the levels. On the other hand, if the lasers are tuned outside the Doppler width of the individual transitions, narrow resonances are possible only if condition (3) is satisfied. In that case, *all* atoms contribute equally to line-shape formation, and the narrowness of the line is due to a *cancellation* of Doppler shifts. Consequently, Eq. (3) will be referred to as the condition for Doppler cancellation to distinguish it from more general Doppler-free criteria.

III. LINE SHAPE—NO COLLISIONS

The wave function for the ith active atom is given by

$$\psi^i(\vec{r}_i, \vec{R}_i, t) = \sum_{\alpha=1}^{3} \sum_m A^i_{\alpha m}(\vec{R}_i, t)\, \psi_{\alpha m}(\vec{r}_i) , \quad (4)$$

where $\vec{r}_i$ represents all relative electronic coordinates of atom i, $\vec{R}_i$ is the center-of-mass coordinate of atom i, α is one of the states shown in Fig. 1, m represents a sublevel of state α, $\psi_{\alpha m}(\vec{r}_i)$ are free-atom electronic eigenfunctions, and the $A^i_{\alpha m}(\vec{R}_i, t)$ represent probability amplitudes. The sum over m covers all the degenerate sublevels of each state α. It will be necessary to perform the calculation in terms of density matrix elements rather than probability amplitudes once collisions are introduced. Macroscopic density matrix elements $\rho_{\alpha m:\alpha' m'}$ are defined as

$$\rho_{\alpha m:\alpha' m'}(\vec{R}, t) = \sum_i A^i_{\alpha m}(\vec{R}, t) A^i_{\alpha' m'}(\vec{R}, t)^* , \quad (5)$$

such that

$$\int \sum_{\alpha m} \rho_{\alpha m:\alpha m}(\vec{R}, t)\, d^3R$$

is just the total number of active atoms. Instead of using the purely quantum-mechanical elements $\rho_{\alpha m:\alpha' m'}(\vec{R}, t)$ it is possible[3] to introduce density matrix elements in classical phase space, $\rho_{\alpha m:\alpha' m'}(\vec{R}, \vec{v}, t)$. The equation of motion for these elements follows directly from an appropriate limit of the Schrödinger equation in which the center-of-mass motion is treated classically.[3] This equation,[3,4]

$$\begin{aligned}\frac{\partial \rho_{\alpha m:\alpha' m'}(\vec{R}, \vec{v}, t)}{\partial t} &= -\vec{v}\cdot\vec{\nabla}\rho_{\alpha m:\alpha' m'}(\vec{R}, \vec{v}, t) + \lambda(\vec{v})\,\delta_{\alpha,1}\,\delta_{\alpha',1}\,\delta_{m,m'} \\ &\quad - \gamma_{\alpha\alpha'}\rho_{\alpha m:\alpha' m'}(\vec{R}, \vec{v}, t) \\ &\quad + (i\hbar)^{-1}[H_0 + V(\vec{R}, t), \rho(\vec{R}, \vec{v}, t)]_{\alpha m:\alpha m'} , \end{aligned} \quad (6)$$

has an intuitive form. The contributions to $\partial\rho_{\alpha m:\alpha' m'}(\vec{R}, \vec{v}, t)/\partial t$ are (a) a convective flow term $-\vec{v}\cdot\vec{\nabla}\rho_{\alpha m:\alpha' m'}(\vec{R}, \vec{v}, t)$, (b) a rate density $\lambda(\vec{v})$ providing an incoherent uniform pumping of all sublevels of level 1, (c) a phenomenological loss term $-\gamma_{\alpha\alpha'}\rho_{\alpha m:\alpha' m'}(\vec{R}, \vec{v}, t)$, where the decay parameters

$$\gamma_{\alpha\alpha'} = \tfrac{1}{2}(\gamma_\alpha + \gamma_{\alpha'}) \quad (7)$$

are m independent, (d) the change in $\rho_{\alpha m:\alpha' m'}$ owing to the free-atom Hamiltonian H_0,

$$(i\hbar)^{-1}[H_0, \rho(\vec{R}, \vec{v}, t)]_{\alpha m:\alpha' m'} = -i\omega_{\alpha\alpha'}\rho_{\alpha m:\alpha' m'}(\vec{R}, \vec{v}, t) , \quad (8)$$

with

$$\omega_{\alpha\alpha'} = (E_\alpha - E_{\alpha'})/\hbar \quad (9)$$

and E_α the free-atom eigenenergy of state α, and (e) the change in $\rho_{\alpha m:\alpha' m'}$ owing to the atom-field interaction

$$(i\hbar)^{-1}[V(\vec{R}, t), \rho(\vec{R}, \vec{v}, t)]_{\alpha m:\alpha' m'} . \quad (10)$$

The atom-field interaction Hamiltonian $V(\vec{r}, \vec{R}, t)$ is given by

$$V(\vec{r}, \vec{R}, t) = -e\vec{r}\cdot[\vec{E}_1(\vec{R}, t) + \vec{E}_2(\vec{R}, t)] , \quad (11)$$

so that the matrix elements needed in (10) are simply

$$V_{\alpha m:\alpha' m'}(\vec{R}, t) = -e\vec{r}_{\alpha m:\alpha' m'}\cdot[\vec{E}_1(\vec{R}, t) + \vec{E}_2(\vec{R}, t)], \quad (12)$$

where

$$\vec{r}_{\alpha m:\alpha' m'} = \int \psi_{\alpha m}(\vec{r})^*\, \vec{r}\, \psi_{\alpha' m'}(\vec{r})\, d^3r . \quad (13)$$

Since the pumping is isotropic and each of the traveling-wave fields is assumed to drive only one transition, it is possible to find stationary solutions to Eqs. (6) if the rotating-wave approximation is made (neglect of antiresonance terms). Writing

$$\rho_{1m:2m'}(\vec{R}, \vec{v}, t) = \tilde{\rho}_{1m:2m'}(\vec{v}) \exp[-i(\vec{k}_1\cdot\vec{R} - \Omega_1 t)], \quad (14a)$$

$$\rho_{2m:3m'}(\vec{R},\vec{v},t)=\tilde{\rho}_{2m:3m'}(\vec{v})\exp[-i(\vec{k}_2\cdot\vec{R}-\Omega_2 t)], \quad (14b)$$

$$\rho_{1m:3m'}(\vec{R},\vec{v},t)=\tilde{\rho}_{1m:3m'}(\vec{v})\exp\{-i[(\vec{k}_1+\vec{k}_2)\cdot\vec{R}-(\Omega_1+\Omega_2)t]\}, \quad (14c)$$

$$\rho_{\alpha m:\alpha m'}(\vec{R},\vec{v},t)=\tilde{\rho}_{\alpha m:\alpha m'}(\vec{v}), \quad (14d)$$

and noting that

$$\rho_{\alpha m:\alpha' m'}=\rho^*_{\alpha' m':\alpha m}, \quad \tilde{\rho}_{\alpha m:\alpha' m'}=\tilde{\rho}^*_{\alpha' m':\alpha m}, \quad (15)$$

one can substitute Eqs. (14) into (6), employ the rotating-wave approximation, use Eqs. (1), (8), and (12), and obtain the following set of equations for the steady-state quantities $\tilde{\rho}_{\alpha m:\alpha' m'}$:

$$\gamma_1\tilde{\rho}_{1m:1m'}(\vec{v})=i\chi^{(1)}_{2p:1m}\tilde{\rho}_{2p:1m'}(\vec{v})-i\chi^{(1)}_{2p:1m'}\tilde{\rho}_{1m:2p}(\vec{v})+\lambda(\vec{v})\delta_{m,m'}, \quad (16a)$$

$$\gamma_2\tilde{\rho}_{2m:2m'}(\vec{v})=i\chi^{(1)}_{2m:1p}\tilde{\rho}_{1p:2m'}(\vec{v})-i\chi^{(1)*}_{2m':1p}\tilde{\rho}_{2m:1p}(\vec{v})+i\chi^{(2)*}_{3p:2m}\tilde{\rho}_{3p:2m'}(\vec{v})-i\chi^{(2)}_{3p:2m'}\tilde{\rho}_{2m:3p}(\vec{v}), \quad (16b)$$

$$\gamma_3\tilde{\rho}_{3m:3m'}(\vec{v})=i\chi^{(2)}_{3m:2p}\tilde{\rho}_{2p:3m'}(\vec{v})-i\chi^{(2)*}_{3m':2p}\tilde{\rho}_{3m:2p}(\vec{v}), \quad (16c)$$

$$[\gamma_{12}-i\delta_{21}(\vec{v})]\tilde{\rho}_{1m:2m'}(\vec{v})=i\chi^{(1)*}_{2p:1m}\tilde{\rho}_{2p:2m'}(\vec{v})-i\chi^{(1)*}_{2m':1p}\tilde{\rho}_{1m:1p}(\vec{v})-i\chi^{(2)}_{3p:2m'}\tilde{\rho}_{1m:3p}(\vec{v}), \quad (16d)$$

$$[\gamma_{23}-i\delta_{32}(\vec{v})]\tilde{\rho}_{2m:3m'}(\vec{v})=i\chi^{(2)*}_{3p:2m}\tilde{\rho}_{3p:3m'}(\vec{v})-i\chi^{(2)*}_{3m':2p}\tilde{\rho}_{2m:2p}(\vec{v})+i\chi^{(1)}_{2m:1p}\tilde{\rho}_{1p:3m'}(\vec{v}), \quad (16e)$$

$$[\gamma_{13}-i\delta_{31}(\vec{v})]\tilde{\rho}_{1m:3m'}(\vec{v})=i\chi^{(1)*}_{2p:1m}\tilde{\rho}_{2p:3m'}(\vec{v})-i\chi^{(2)*}_{3m':2p}\tilde{\rho}_{1m:2p}(\vec{v}), \quad (16f)$$

where

$$\chi^{(1)}_{2p:1m}=e\vec{r}_{2p:1m}\cdot\vec{\mathcal{E}}_1/2\hbar, \quad (17a)$$

$$\chi^{(2)}_{3p:2m}=e\vec{r}_{3p:2m}\cdot\vec{\mathcal{E}}_2/2\hbar, \quad (17b)$$

$$\delta_{21}(\vec{v})=\omega_{21}-\Omega_1+\vec{k}_1\cdot\vec{v}, \quad (18a)$$

$$\delta_{32}(\vec{v})=\omega_{32}-\Omega_2+\vec{k}_2\cdot\vec{v}, \quad (18b)$$

$$\delta_{31}(\vec{v})=\delta_{21}(\vec{v})+\delta_{32}(\vec{v})=\omega_{31}-(\Omega_1+\Omega_2)+(\vec{k}_1+\vec{k}_2)\cdot\vec{v}. \quad (18c)$$

In writing Eqs. (16), terms corresponding to field $\vec{E}_1$ driving the $2\leftrightarrow 3$ transition and $\vec{E}_2$ driving the $1\leftrightarrow 2$ transition have been omitted, and a summation convention is implicit in which *all* repeated latin indices are summed unless otherwise specified (the sum is over the magnetic substates).

Equations (16) represent a set of algebraic equations which may be solved exactly.[20] However, we are interested only in a perturbative solution. The quantity of experimental interest is the upper-state population, or, to allow for a somewhat more general experimental situation,[21] a set of values for all upper-state density matrix elements. In perturbation theory, the upper state is reached by the two types of paths depicted below:

$$\rho_{1:1}\rightarrow\begin{Bmatrix}\rho_{1:2}\\ \rho_{2:1}\end{Bmatrix}\rightarrow\begin{Bmatrix}\rho_{1:3}\\ \rho_{3:1}\end{Bmatrix}\rightarrow\rho_{3:3}\leftarrow\begin{Bmatrix}\rho_{2:3}\\ \rho_{3:2}\end{Bmatrix}\leftarrow\rho_{2:2}. \quad (19)$$

The upper path does not involve any intermediate-state population and is commonly referred to as a two-quantum process, while the lower path is usually labeled a stepwise excitation, since the intermediate-state population explicitly appears. This separation is somewhat artificial, since there is no way to separate out the contributions from either path in the absence of collisions. It is clear that had the calculation been done with probability *amplitudes* the breakup into two-quantum and stepwise excitation would not naturally occur. There will be some cases where the two-quantum contribution is dominant, but, in general, both contributions influence the line shape.

The value of $\tilde{\rho}_{3m:3m'}(\vec{v})$ follows from a straightforward perturbation calculation and one easily finds

$$\tilde{\rho}_{3m:3m'}(\vec{v})=\tilde{\rho}^{TQ}_{3m:3m'}(\vec{v})+\tilde{\rho}^{SW}_{3m:3m'}(\vec{v}), \quad (20)$$

with

$$\tilde{\rho}^{TQ}_{3m:3m'}(\vec{v})=2\lambda(\vec{v})A_{mm'}[\gamma_{12}\gamma_{23}\gamma_{13}-\gamma_{23}\delta_{31}(\vec{v})\delta_{21}(\vec{v})-\gamma_{12}\delta_{31}(\vec{v})\delta_{32}(\vec{v})-\gamma_{13}\delta_{21}(\vec{v})\delta_{32}(\vec{v})]\times\mathcal{L}_{13}(\vec{v})\mathcal{L}_{23}(\vec{v})\mathcal{L}_{12}(\vec{v})/(\gamma_3\gamma_1), \quad (21a)$$

$$\tilde{\rho}^{SW}_{3m:3m'}(\vec{v})=4\lambda(\vec{v})A_{mm'}\gamma_{12}\gamma_{23}\mathcal{L}_{12}(\vec{v})\mathcal{L}_{23}(\vec{v})/\gamma_2\gamma_3\gamma_1, \quad (21b)$$

where

$$A_{mm'}=\chi^{(1)}_{2p:1s}\chi^{(1)*}_{2r:1s}\chi^{(2)}_{3m:2p}\chi^{(2)*}_{3m':2r}, \quad (21c)$$

and the Lorentzians

$$\mathcal{L}_{ij}(\vec{v})=\{(\gamma_{ij})^2+[\delta_{ji}(\vec{v})]^2\}^{-1}. \quad (22)$$

The quantities $\tilde{\rho}^{TQ}_{3m:3m'}$ and $\tilde{\rho}^{SW}_{3m:3m'}$ represent the contributions to $\tilde{\rho}_{3m:3m'}$ from the upper and lower paths, respectively, shown in (19). This separation will be useful when collisions are introduced in Sec. IV. Note that Eq. (21b) is simply a product

of absorption cross sections for the $1 \rightarrow 2$ and $2 \rightarrow 3$ transitions.

By combining Eqs. (20) and (21) and making use of Eqs. (7) and (18), one can write $\tilde{\rho}_{3m:3m'}$ in the simplified form

$$\begin{aligned}\tilde{\rho}_{3m:3m'}(\vec{v}) = \lambda(\vec{v}) A_{mm'} (\gamma_1 \gamma_2 \gamma_3)^{-1} \\ \times [\gamma_1 \gamma_3 \mathcal{L}_{12}(\vec{v}) \mathcal{L}_{23}(\vec{v}) \\ + \gamma_1 \gamma_2 \mathcal{L}_{23}(\vec{v}) \mathcal{L}_{13}(\vec{v}) + \gamma_2 \gamma_3 \mathcal{L}_{12}(\vec{v}) \mathcal{L}_{13}(\vec{v}) \\ + \gamma_1 \gamma_2 \gamma_3 (\gamma_1 + \gamma_2 + \gamma_3) \mathcal{L}_{12}(\vec{v}) \mathcal{L}_{23}(\vec{v}) \mathcal{L}_{13}(\vec{v})] .\end{aligned} \tag{23}$$

When integrated over velocity with some appropriate $\lambda(\vec{v})$, the line shape

$$I_{mm'} = \int \tilde{\rho}_{3m:3m'}(\vec{v})\, d^3v \tag{24}$$

is the general result for excitation involving two photons and is analogous to the result obtained by Omont, Smith, and Cooper[22] for the related problem of Raman scattering. While Eq. (23) will not be discussed in detail, it may be noted that in the limit of well-defined upper and lower states ($\gamma_1 \sim 0$, $\gamma_3 \sim 0$) the velocity-dependent line shape (23) becomes proportional to a δ function $\delta(\delta_{31}(\vec{v}))$, in agreement with the conclusions of Heitler.[18,23]

An explicit evaluation of Eq. (24) will be made for the practically important case in which level 1 is a ground state. Writing the excitation density

$$\lambda(\vec{v}) = \lambda W(\vec{v}) , \tag{25a}$$

where

$$W(\vec{v}) = (\pi u^2)^{-3/2} e^{-v^2/u^2} \tag{25b}$$

is the assumed Maxwellian velocity distribution and λ is the excitation rate per unit volume, and taking the limit

$$\gamma_1 \sim 0, \quad \lambda \sim 0, \quad \lambda/\gamma_1 = \text{const} = N_0 , \tag{26}$$

one obtains the line shape from Eqs. (23) and (24) as

$$\begin{aligned}I_{mm'} = N_0 A_{mm'} \int d^3v\, W(\vec{v}) [(\gamma_{12})^2 + (\Delta_{21} - \vec{k}_1 \cdot \vec{v})^2]^{-1} \\ \times \{(\gamma_{13})^2 + [\Delta_{31} - (\vec{k}_1 + \vec{k}_2) \cdot \vec{v}]^2\}^{-1} ,\end{aligned} \tag{27}$$

where the definitions (18) and (22) have been used and the detunings Δ are defined as

$$\begin{aligned}&\Delta_{21} = \Omega_1 - \omega_{21}, \quad \Delta_{32} = \Omega_3 - \omega_{32} , \\ &\Delta_{31} = \Omega_1 + \Omega_2 - (\omega_{21} + \omega_{32}) .\end{aligned} \tag{28}$$

Equation (27) may be further reduced if the Doppler cancellation condition [Eq. (3)] is applicable. In that limit,

$$I_{mm'} = N_0 A_{mm'} [(\gamma_{13})^2 + (\Delta_{31})^2]^{-1} \int d^3v\, W(\vec{v}) [(\gamma_{12})^2 + (\Delta_{21} - \vec{k} \cdot \vec{v})^2]^{-1} , \tag{29a}$$

$$\sim N_0 A_{mm'} [(\gamma_{13})^2 + (\Delta_{31})^2]^{-1} \begin{cases} \pi^{1/2} (ku\gamma_{12})^{-1} \exp[-(\Omega_1/ku)^2], & |\Delta_{21}| < ku , \\ (\Delta_{21})^{-2}, & |\Delta_{21}| \gg ku , \end{cases} \tag{29b}$$

where we have assumed the Doppler limit $\gamma_i \ll ku$ in writing Eqs. (29b). In Fig. 2 the line shape is shown for fixed Δ_{21} and Δ_{32} varied. There is a single sharp resonance with a half width at half-maximum (HWHM) of γ_{13} at $\Delta_{31} = \Delta_{21} + \Delta_{32} = 0$. The absence of another resonance is due to the fact that level 1 has zero width. If the lower laser frequency is varied with Δ_{32} fixed, then the line shape as a function of Δ_{21} would have *two* resonances, a sharp one at $\Delta_{31} = 0$ ($\Delta_{21} = -\Delta_{32}$) and a Doppler-broadened one at $\Delta_{21} = 0$. The discussion will be limited to the case of Δ_{21} fixed. More general line-shape expressions, valid when Eqs. (3) and (26) no longer hold, are given in Appendix B.

IV. LINE SHAPE–COLLISIONS

In Appendix A, a formal theory of collision effects appropriate to the level scheme of Fig. 1 is developed. The results give expressions for the collisional time rate of change of the various density matrix elements. These expressions are quite complex, in general, and do not even lend themselves to a simple interpretation in terms of "phase-interrupting" and "velocity-changing" collisions. There are, however, certain physical situations in which the equations take on a simplified form. A common case of practical interest is one where levels 1, 2, and 3 represent different electronic states of an atom. Assuming these levels experience reasonably different collisional interactions with perturber atoms, collisional changes for density matrix elements of the form $\rho_{\alpha m:\alpha' m'}$, with $\alpha' \neq \alpha$, will involve forward scattering only, owing to quantum-mechanical interference effects.[2-4] *Within* a given state α, collisions can both reorient the magnetic sublevels and cause a change in atomic velocity.

In light of the above comments, the collisional change in density matrix elements may be written

$$\left(\frac{\partial \bar{\rho}_{\alpha m:\alpha' m'}(\vec{R},\vec{v},t)}{\partial t}\right)_{\text{coll}} = -\gamma^{ph}_{\alpha m:\alpha' m'}(\vec{v})\bar{\rho}_{\alpha m:\alpha' m'}(\vec{R},\vec{v},t), \qquad \alpha \neq \alpha', \quad \text{no sum}, \tag{30a}$$

$$\left(\frac{\partial \bar{\rho}_{\alpha m:\alpha m'}(\vec{R},\vec{v},t)}{\partial t}\right)_{\text{coll}} = -R^{nn'}_{mm'}(\vec{v};\alpha)\bar{\rho}_{\alpha n:\alpha n'}(\vec{R},\vec{v},t) + \int d^3v' W^{mn'}_{mm'}(\vec{v}'\to\vec{v};\alpha)\bar{\rho}_{\alpha n:\alpha n'}(\vec{R},\vec{v}',t). \tag{30b}$$

The parameters $\gamma^{ph}_{\alpha m:\alpha m'}(\vec{v})$, $R^{mn'}_{mm'}(\vec{v},\alpha)$, and $W^{nn'}_{mm'}(\vec{v}'\to\vec{v},\alpha)$ are defined in Appendix A. They depend on various scattering amplitudes and are linearly proportional to pressure. Equation (30a) reflects the fact that because of the assumed state-dependent collision interaction collisions are solely of a phase-interrupting nature for density matrix elements coupling different electronic states α and α'. The complex quantity γ^{ph} gives rise to the familiar shift and broadening of spectral profiles. The rate $R^{nn'}_{mm'}(\vec{v};\vec{\alpha})$ and kernel $W^{nn'}_{mm'}(\vec{v}';\vec{\alpha})$ appearing in Eq. (30b) are complex and, in general, cannot be given a simple interpretation. They represent an unseparable combination of magnetic reorientation and velocity-changing effects within a given state α.

The right-hand side (rhs) of Eqs. (30) should be added to the rhs of Eqs. (16) and the set of equations solved to determine the excitation line shape in the presence of collisions. This program is carried out in Appendix A and the line shape is

$$I = \rho^{TQ}_{3m:3m} + \rho^{SW}_{3m:3m}, \tag{31}$$

where

$$\rho^{TQ}_{3m:3m} = N_0\gamma_3^{-1}A^{hjqh}_{sjqs}\int d^3v_0\,\mathfrak{D}_{2s:3q}(\vec{v}_0-\vec{k}_2)\mathfrak{D}_{1j:3q}(\vec{v}_0,-\vec{k}_1-\vec{k}_2)\mathfrak{D}_{1j:2h}(\vec{v}_0,-\vec{k}_1)W(\vec{v}_0) + \text{c.c.} \tag{32a}$$

and

$$\rho^{SW}_{3m:3m} = N_0\gamma_3^{-1}A^{hjqr}_{sjqp}\int d^3v\int d^3v_0\,[\mathfrak{D}_{2p:3q}(\vec{v},-\vec{k}_2)+\mathfrak{D}_{2r:3q}(\vec{v},-\vec{k}_2)^*] \times G^{sh}_{pr}(\vec{v}_0\to\vec{v};2)[\mathfrak{D}_{1j:2h}(\vec{v}_0,-\vec{k}_1)+\mathfrak{D}_{1j:2s}(\vec{v}_0,-\vec{k}_1)^*]W(\vec{v}_0) \tag{32b}$$

correspond to Eqs. (21) modified to include collisions and integrated over velocity. The quantities appearing in Eqs. (32) are $N_0 = \lambda/\gamma_1$,

$$A^{hmnr}_{sjqp} = \chi^{(1)}_{2s:1j}\chi^{(1)*}_{2h:1m}\chi^{(2)}_{3q:2p}\chi^{(2)*}_{3n:2r} \tag{33}$$

containing the applied field intensities,

$$\mathfrak{D}_{\alpha m:\alpha' m'}(\vec{v},\vec{k}) = [\gamma_{\alpha\alpha'} - i\Delta_{\alpha'\alpha} + i\vec{k}\cdot\vec{v} + \gamma^{ph}_{\alpha m:\alpha' m'}(\vec{v})]^{-1}, \tag{34}$$

which is a resonance denominator containing the detuning $\Delta_{\alpha\beta}$ defined in Eq. (28) and a collisional width and shift contribution $\gamma^{ph}_{\alpha m:\alpha' m'}(\vec{v})$, the propagator $G^{sh}_{pr}(\vec{v}'\to\vec{v};2)$ defined as a solution to the equation

$$\gamma_2 G^{sh}_{pr}(\vec{v}'\to\vec{v};2) = -R^{mn}_{pr}(\vec{v};2)G^{sh}_{mn}(\vec{v}'\to\vec{v};2) + \int d^3v_1 W^{mn}_{pr}(\vec{v}_1\to\vec{v};2)G^{sh}_{mn}(\vec{v}'\to\vec{v}_1;2) + \delta(\vec{v}'-\vec{v})\delta_{p,s}\delta_{r,h}, \tag{35}$$

where R^{mn}_{pr} and W^{mn}_{pr} are the complex rates and kernel given in Eq. (30b), and the Maxwellian distribution $W(\vec{v})$. For simplicity, the level-3 population rather than an arbitrary density matrix element has been displayed—the more general formula appears in Appendix A.

Equations (32) can be easily understood in light of the above comments concerning the collision model which has been adopted and the perturbation chain depicted in expression (19). Collisions distinguish the upper two-quantum (TQ) chain from the lower stepwise (SW) one. In both chains, unpolarized atoms start in level 1 with a Maxwellian velocity distribution. Since this is an *equilibrium* distribution for the atoms, collisions will not alter it. In the TQ chain, the fields then create off-diagonal density matrix elements ρ_{12}, ρ_{13}, and ρ_{23}. The net effect of collisions on such density matrix elements in the model adopted is to provide a complex decay parameter $\gamma^{ph}_{\alpha\alpha'}$ but no velocity changes. This accounts for the presence of $\mathfrak{D}_{12}(\vec{v}_0)$, $\mathfrak{D}_{13}(\vec{v}_0)$, and $\mathfrak{D}_{23}(\vec{v}_0)$ in Eq. (32a). On the other hand, although ρ_{12} and ρ_{23} also appear in the SW chain, the intermediate term is now ρ_{22}.

Collisions are phase interrupting in their effect on ρ_{12} and ρ_{23}, but will, in general, alter $\rho_{2m;2m'}(\vec{v})$ with an unseparable combination of magnetic reorientation and velocity-changing effects. Consequently, one finds the product $\mathfrak{D}_{12}(\vec{v}_0) \times G^{sh}_{pr}(\vec{v}_0 \to \vec{v}; 2)\mathfrak{D}_{23}(\vec{v})$ appearing in Eq. (32b). In both chains the final step involves the total upper-state population, which is unchanged by collisions. The implications of the difference in the nature of the TQ and SW chains will be discussed in the following sections.

It should be noted that the evaluation of the line shape [Eqs. (32)] represents a formidable problem even for the relatively simple collision model chosen. To determine the propagator $G^{sh}_{pr}(\vec{v}_0 \to \vec{v}_1, 2)$ needed in Eq. (32), one must solve Eq. (35) and, to solve Eq. (35), one must have values for the rate $R^{mn}_{pr}(\vec{v}; 2)$ and kernel $W^{mn}_{pr}(\vec{v}_1 \to \vec{v}_2; 2)$. Although formal expressions for these quantities are given in Appendix A and these expressions may be simplified by symmetry considerations in some cases, one is usually forced into adopting some phenomenological forms for these rates and kernels. Specific examples are given below.

V. NATURE OF THE LINE SHAPE

A. No degeneracy

If levels 1, 2, and 3 are nondegenerate, Eqs. (32) take on an especially simple form. Dropping all magnetic substate indices and using definitions (33) and (34), one can reduce Eqs. (32) to

$$\rho_{33}^{TQ} = N_0\gamma_3^{-1}A \int d^3v_0 \mathfrak{D}_{23}(\vec{v}_0, -\vec{k}_2)\mathfrak{D}_{13}(\vec{v}_0, -\vec{k}_1 - \vec{k}_2) \times \mathfrak{D}_{12}(\vec{v}_0, -\vec{k}_1)W(\vec{v}_0) + \text{c.c.}, \tag{36a}$$

$$\rho_{33}^{SW} = 2N_0\gamma_3^{-1}A \times \int d^3v \int d^3v_0 [\gamma_{23} + \Gamma^{ph}_{23}(\vec{v})]\mathfrak{L}^{ph}_{23}(\vec{v})G(\vec{v}_0 \to \vec{v}; 2) \times [\gamma_{12} + \Gamma^{ph}_{12}(\vec{v}_0)]\mathfrak{L}^{ph}_{12}(\vec{v}_0)W(\vec{v}_0), \tag{36b}$$

where the collision-modified Lorentzians are given by

$$\mathfrak{L}^{ph}_{ij}(\vec{v}) = [\gamma_{ij} + \Gamma^{ph}_{ij}(\vec{v})]^2 + [\delta_{ji}(\vec{v}) - \mathcal{S}^{ph}_{ij}(\vec{v})]^2, \tag{37}$$

$$\Gamma^{ph}_{ij}(\vec{v}) = \text{Re}\gamma^{ph}_{ij}(\vec{v}), \quad \mathcal{S}^{ph}_{ij}(\vec{v}) = \text{Im}\gamma^{ph}_{ij}(\vec{v}), \tag{38}$$

$$A = |\chi^{(1)}_{21}|^2 |\chi^{(2)}_{32}|^2. \tag{39}$$

The propagator G now satisfies the equation

$$\gamma_2 G(\vec{v}_0 \to \vec{v}; 2) = -\Gamma(\vec{v}; 2)G(\vec{v}_0 \to \vec{v}; 2) + \int d^3v_1 W(\vec{v}_1 \to \vec{v}; 2)G(\vec{v}_0 \to \vec{v}_1; 2) + \delta(\vec{v}_0 - \vec{v}), \tag{40}$$

with *real* kernel $W(\vec{v}_1 \to \vec{v}; 2)$ and rate $\Gamma(\vec{v}; 2)$ for velocity-changing collisions [$\Gamma(\vec{v}; 2) = \int W(\vec{v} \to \vec{v}'; 2) \times d^3v'$], and the $\mathfrak{D}_{ij}$ are defined by Eq. (34). The only difference from the no-collision TQ contribution (21a) is that the replacements $\gamma_{ij} \to \gamma_{ij} + \Gamma^{ph}_{ij}(\vec{v})$ and $\delta_{ji} \to \delta_{ji} - \mathcal{S}^{ph}_{ij}(\vec{v})$, have been made, indicating a collisional contribution to the decay of ρ_{ij} and a collisional frequency shift. On the other hand, the SW contribution can now be interpreted as arising from a collisionally modified absorption to level 2 followed by velocity-changing collisions in level 2 followed by a collisionally modified absorption to level 3. Collisions have resulted in a fundamentally different form for the TQ and SW chains.

Once a choice for $W(\vec{v}_0 \to \vec{v}; 2)$ is made, Eq. (40) may be solved for $G(\vec{v}_0 \to \vec{v}; 2)$ and the general expressions (36) numerically integrated. However, for the specific example that has been previously considered, some analytic progress is possible. Adopting the Doppler cancellation condition (3) and neglecting the $\vec{v}$ dependence in γ^{ph}_{ij} (which is generally a good first approximation), Eqs. (36) may be written

$$\rho_{33}^{TQ} = 2N_0\gamma_3^{-1}A[(\tilde{\gamma}_{13})^2 + (\tilde{\delta}_{31})^2]^{-1} \int d^3v_0 [\tilde{\gamma}_{12}\tilde{\gamma}_{23}\tilde{\gamma}_{13} - \tilde{\gamma}_{23}\tilde{\delta}_{31}\tilde{\delta}_{21}(\vec{v}) - \tilde{\gamma}_{12}\delta_{31}\delta_{32}(\vec{v}) - \tilde{\gamma}_{13}\tilde{\delta}_{21}(\vec{v})\tilde{\delta}_{32}(\vec{v})]\mathfrak{L}^{ph}_{23}(\vec{v}_0)\mathfrak{L}^{ph}_{12}(\vec{v}_0)W(\vec{v}_0), \tag{41a}$$

$$\rho_{33}^{SW} = 4N_0\gamma_3^{-1}A\tilde{\gamma}_{23}\tilde{\gamma}_{12} \int d^3v_0 \int d^3v\, \mathfrak{L}^{ph}_{23}(\vec{v})G(\vec{v}_0 \to \vec{v}; 2)\mathfrak{L}^{ph}_{12}(\vec{v}_0)W(\vec{v}_0), \tag{41b}$$

where

$$\tilde{\gamma}_{ij} = \gamma_{ij} + \Gamma^{ph}_{ij}, \tag{42a}$$

$$\tilde{\delta}_{21}(\vec{v}) = -\tilde{\Delta}_{21} + \vec{k}_1 \cdot \vec{v}, \quad \tilde{\delta}_{32}(\vec{v}) = -\tilde{\Delta}_{32} + \vec{k}_2 \cdot \vec{v}, \tag{42b}$$

$$\tilde{\delta}_{31} = \tilde{\Delta}_{31}, \tag{42c}$$

$$\tilde{\Delta}_{21} = \Delta_{21} + \mathcal{S}^{ph}_{12}, \quad \tilde{\Delta}_{32} = \Delta_{32} + \mathcal{S}^{ph}_{23}, \tag{43a}$$

$$\tilde{\Delta}_{31} = \Delta_{21} + \Delta_{32} + \mathcal{S}^{ph}_{13}, \tag{43b}$$

and the detunings Δ_{ij} are defined in (28).

For the propagator $G(\vec{v}_0 \to \vec{v}; 2)$, we choose an extremely simple phenomenological two-parameter expression

$$G(\vec{v}_0 \to \vec{v}; 2) = (\gamma_2)^{-1}\{\alpha\delta(\vec{v} - \vec{v}_0) + (1-\alpha)[\pi(1-r^2)u^2]^{-3/2} \times \exp[-(\vec{v} - r\vec{v}_0)^2/(1-r^2)u^2]\}, \tag{44a}$$

where

$$r = \beta^{1/\alpha}, \tag{44b}$$

$$\alpha = \gamma_2/[\gamma_2 + \Gamma(2)]; \tag{45}$$

$\Gamma(2)$ is the rate for velocity-changing collisions in level 2, β is a constant between zero and one, and u is the thermal speed appearing in Eq. (25b). Equation (44) may be easily understood if one realizes that the propagator simply determines the change undergone by a δ-function velocity distribution in the time $\tau_2 = (\gamma_2)^{-1}$. Since the parameter α gives the fraction of atoms that do not undergo collisions in the interval τ_2, the first term in (44a) represents the contribution from atoms which have not experienced velocity-changing collisions. The parameter β characterizes the strength of a single collision, with $\beta = 1$ corresponding to a weak collision and $\beta = 0$ corresponding to a strong thermalizing collision. Consequently, the second term in (44a) represents the contribution from atoms which have their velocity changed from a δ function $\delta(\vec{v} - \vec{v}_0)$ to a distribution of velocities centered at $\vec{v} = r\vec{v}_0$ with width $(1-r^2)^{1/2}ku$. The parameter r, defined in (44b), represents an average velocity-changing effect for the many single collisions which may occur in a time interval τ_2.[24] Although simple in form, $G(\vec{v}_0 \to \vec{v}; 2)$ has the needed properties that its integral over $\vec{v}$ gives $(\gamma_2)^{-1}$ and

$$\int d^3v_0\, G(\vec{v}_0 \to \vec{v}; 2) W(\vec{v}_0) = W(\vec{v})/\gamma_2, \tag{46}$$

expressing the fact that collisions will not alter an equilibrium distribution.

The line shape (31) may now be evaluated as a function of Δ_{32} for fixed Δ_{21}. In all the calculations, the Doppler limit

$$ku \gg \tilde{\gamma}_{ij}, |\mathcal{S}_{ij}^{ph}| \tag{47}$$

will be taken to hold.

1. $|\Delta_{21}| \gg ku$

For such values of Δ_{21}, $\delta_{21}(\vec{v}) \approx -\Delta_{21}$ and $\mathcal{L}_{12}^{ph}(\vec{v}) \approx (\Delta_{21})^{-2}$. Using Eqs. (41)–(43), (46), and (47), one obtains the line shape (31) as

$$I = 2N_0A(\gamma_3)^{-1}(\Delta_{21})^{-2}\int d^3v_0\, W(\vec{v}_0)\mathcal{L}_{23}^{ph}(\vec{v}_0)\{[\tilde{\gamma}_{12}\tilde{\gamma}_{23}\tilde{\gamma}_{13} + \tilde{\gamma}_{23}\tilde{\delta}_{31}\Delta_{21} - \tilde{\gamma}_{12}\tilde{\delta}_{31}\tilde{\delta}_{32}(\vec{v}) + \tilde{\gamma}_{13}\Delta_{21}\tilde{\delta}_{32}(\vec{v})][(\tilde{\gamma}_{13})^2 + (\tilde{\delta}_{31})^2]^{-1} + \tilde{\gamma}_{12}\tilde{\gamma}_{23}(\gamma_2)^{-1}\}. \tag{48}$$

Velocity-changing collisions are unimportant here, since the detuning Δ_{21} is so large that each velocity subset of atoms is essentially equivalent in the $1 \to 2$ absorption of the SW chain. The line shape (48) has a sharp resonance for $\Delta_{32} \approx -\Delta_{21}$ and a broad one at $\Delta_{32} \approx 0$. Near these two resonances, Eq. (48) may be written

$$I = \frac{2N_0A}{\gamma_3(\Delta_{21})^2}\left(\frac{\tilde{\gamma}_{13}}{(\tilde{\gamma}_{13})^2 + (\Delta_{32} + \Delta_{21} + \mathcal{S}_{13}^{ph})^2}\right), \quad \text{for } \Delta_{32} \approx -\Delta_{21}, \tag{49a}$$

$$I = \frac{4N_0A\pi^{1/2}}{ku\gamma_3(\Delta_{21})^2}\left(\frac{\Gamma_{12}^{ph}}{\gamma_2}\right)\exp\left[-\left(\frac{\Delta_{32} + \mathcal{S}_{23}^{ph}}{ku}\right)^2\right], \quad \text{for } \Delta_{32} \approx 0, \tag{49b}$$

where, for consistency with Sec. III, we have taken level 1 as a ground state.

The line shape for a detuning $\Delta_{21} = -4.0ku$ is shown in Fig. 3, with variables expressed in dimensionless units obtained by dividing them by the Doppler width ku. For the natural-decay parameters, we have taken $\gamma_1 = 0$, $\gamma_2/ku = 0.03$, and $\gamma_3/ku = 0.02$. The collision parameters depend linearly on the pressure and, to correspond to perturber pressures on the order of several Torr, we have chosen $\Gamma_{12}^{ph}/ku = 0.06$, $\Gamma_{23}^{ph}/ku = 0.08$, $\Gamma_{13}^{ph}/ku = 0.1$, $\mathcal{S}_{12}^{ph} = 0.02$, $\mathcal{S}_{23}^{ph} = 0.04$, and $\mathcal{S}_{13}^{ph} = 0.02$. The line shape and those to follow are normalized so that the corresponding no-collision line shape would have a maximum amplitude of unity. The no-collision line shape, for this case, would be centered at $\Delta_{32} = -\Delta_{21}$, with HWHM of $\gamma_{13}/ku = 0.01$.

The line shape (49) differs from the no-collision result in two ways. First, the sharp resonance arising mainly from the TQ contribution has been shifted, broadened, and decreased in intensity by collisions. Second, one finds a *new* broad resonance at $\Delta_{32} = -\mathcal{S}_{23}^{ph}$ which arises from the fact that collisions have effectively introduced some width into the ground state. The broad resonance represents an expanded frequency range of Δ_{32}

which will give rise to excitation. The ratio of the broad- to narrow-resonance amplitudes is $2\pi^{1/2}(\tilde{\gamma}_{13}/ku)(\Gamma_{12}^{ph}/\gamma_2)<1$ and vanishes for no collisions $\Gamma_{12}^{ph}=0$.

2. $|\Delta_{21}|<ku$

For detunings within the Doppler width, the major contribution to the excitation will be achieved if Δ_{12} and Δ_{32} are chosen such that the same velocity subset of atoms can be resonant with fields $\vec{E}_1$ and $\vec{E}_2$ on the $1\rightarrow 2$ and $2\rightarrow 3$ transitions, respectively. The resonance conditions for individual atom-field interactions are (neglecting collisional shifts)

$$\vec{k}_1\cdot\vec{v}_1=-\Delta_{21},\quad \vec{k}_2\cdot\vec{v}_2\approx-\vec{k}_1\cdot\vec{v}_2=-\Delta_{32}, \tag{50}$$

where $\vec{v}_1$ and $\vec{v}_2$ are the atomic velocities when fields $\vec{E}_1$ and $\vec{E}_2$ interact with the atom and $\vec{k}_2\approx-\vec{k}_1$ in the case under discussion.

Thus in the TQ chain [Eq. (41a)], where velocity-changing collisions do not enter, $\vec{v}_1=\vec{v}_2$ and Eq. (50) will be satisfied if $\Delta_{32}=-\Delta_{21}$. A straightforward evaluation of Eq. (41a) in the Doppler limit (47) leads to the TQ line-shape contribution[25]

$$\rho_{33}^{TQ}=\frac{4\pi^{1/2}N_0A\exp[-(\Delta_{21}+\mathcal{S}_{12}^{ph})^2/(ku)^2]}{ku\gamma_3[(\tilde{\gamma}_{13})^2+(\Delta_{32}+\Delta_{21}+\mathcal{S}_{13}^{ph})^2](\bar{\Gamma}^2+\bar{\Delta}^2)}\times[\bar{\Gamma}\tilde{\gamma}_{13}-\bar{\Delta}(\Delta_{32}+\Delta_{21}+\mathcal{S}_{13}^{ph})], \tag{51a}$$

where

$$\bar{\Gamma}=\tilde{\gamma}_{12}+\tilde{\gamma}_{23}, \tag{51b}$$

$$\bar{\Delta}=\Delta_{32}+\Delta_{21}+\mathcal{S}_{12}^{ph}+\mathcal{S}_{23}^{ph}. \tag{51c}$$

The TQ contribution is slightly asymmetric because of the presence of resonances at both $\Delta_{32}=-\Delta_{21}-\mathcal{S}_{13}^{ph}$ and $\Delta_{32}=-\Delta_{21}-\mathcal{S}_{12}^{ph}-\mathcal{S}_{23}^{ph}$.

In the SW chain [Eq. (41b)], the atomic velocity may be different when fields $\vec{E}_1$ and $\vec{E}_2$ act, as a result of velocity-changing collisions. When Eq. (44) for the propagator is inserted into Eq. (41b), the resulting integral does not have a simple analytic form. However, for a sufficiently large range of the parameter r defined by Eq. (44b), the integral may be approximated in the Doppler limit (47) as

$$\rho_{33}^{SW}=4\pi^{1/2}N_0A(ku\gamma_3)^{-1}\exp[-(\Delta_{21}+\mathcal{S}_{12}^{ph})^2/(ku)^2]\times\left[\frac{\alpha\bar{\Gamma}}{\gamma_2(\bar{\Gamma}^2+\bar{\Delta}^2)}+\frac{(1-\alpha)}{(1-r^2)^{1/2}}\left(\frac{\pi^{1/2}}{ku\gamma_2}\right)\times\exp\left(-\frac{[\Delta_{32}+\mathcal{S}_{23}^{ph}+r(\Delta_{21}+\mathcal{S}_{12}^{ph})]^2}{k^2u^2(1-r^2)}\right)\right]. \tag{52}$$

Equation (52) is not valid for $r=\beta^{1/\alpha}\approx 1$. However, the correct limiting value of ρ_{33}^{SW} for $r\approx 1$ is obtained by setting

$$\alpha=1 \quad \text{if } \beta=1. \tag{53}$$

The SW contribution consists of two parts. The first term represents atoms which have not undergone collisions and has a resonance at $\Delta_{32}=-\Delta_{21}-\mathcal{S}_{12}^{ph}-\mathcal{S}_{23}^{ph}$, which is effectively the resonance condition (50) with $\vec{v}_2=\vec{v}_1$. The second term represents atoms which have effectively had their velocity changed from $\vec{v}_1$ to $\vec{v}_2=r\vec{v}_1$, giving rise to a new resonance condition from Eq. (50) at $\Delta_{32}=-r(\Delta_{21}+\mathcal{S}_{12}^{ph})-\mathcal{S}_{23}^{ph}$. The width of this new resonance is $\approx ku(1-r^2)^{1/2}$ and is a direct manifestation of velocity-changing collisions.

Combining Eqs. (51) and (52) leads to the total line shape for the case $|\Delta_{21}|<ku$,

$$I=4\pi^{1/2}N_0A(ku\gamma_3)^{-1}(\tilde{\gamma}_{13})^{-2}\exp[-(\Delta_{21}+\mathcal{S}_{12}^{ph})^2/(ku)^2]\times\left(\frac{(\tilde{\gamma}_{13})^2(\bar{\Gamma}\tilde{\gamma}_{13}-\bar{\Delta}\tilde{\Delta}_{31})}{[(\tilde{\gamma}_{13})^2+(\tilde{\Delta}_{31})^2](\bar{\Gamma}^2+\bar{\Delta}^2)}+\frac{\alpha\bar{\Gamma}(\tilde{\gamma}_{13})^2}{\gamma_2(\bar{\Gamma}^2+\bar{\Delta}^2)}+(1-\alpha)\pi^{1/2}(1-r^2)^{-1/2}(ku\gamma_2)^{-1}(\tilde{\gamma}_{13})^2\exp[-(\tilde{\Delta}_{32}+r\tilde{\Delta}_{21})^2/(1-r^2)k^2u^2]\right), \tag{54}$$

where $\tilde{\Delta}_{ij}$, $\bar{\Delta}$, and $\bar{\Gamma}$ are defined by Eqs. (43) and (51). The line shape consists of three parts. The first term is the TQ contribution, which, in general, is asymmetric, since $\bar{\Delta}\neq\tilde{\Delta}_{31}$. However, if $\bar{\Gamma}>\tilde{\gamma}_{13}$, the line will possess a nearly Lorentzian peak centered at $\Delta_{32}\approx-\Delta_{21}-\mathcal{S}_{13}^{ph}$, with HWHM of $\tilde{\gamma}_{13}$. The second term is the SW contribution from those atoms which have not undergone collisions before being excited to state 3. It is a Lorentzian centered at $\Delta_{32}=-\Delta_{21}-\mathcal{S}_{12}^{ph}-\mathcal{S}_{23}^{ph}$, with HWHM of $\bar{\Gamma}=\tilde{\gamma}_{12}+\tilde{\gamma}_{23}$, and is usually broader than the TQ term, since $\bar{\Gamma}>\tilde{\gamma}_{13}$ is typical. The detuning giving rise to maximum amplitude is shifted from the corresponding TQ value. The third and final term is the SW contribution and is a Gaussian centered at $\Delta_{32}=-r(\Delta_{21}+\mathcal{S}_{12}^{ph})-\mathcal{S}_{13}^{ph}$, with width $(1-r^2)^{1/2}ku$. The ratio of the amplitudes of each of the terms at their respective maxima is

$$1:\alpha(\tilde{\gamma}_{13}/\gamma_2):(1-\alpha)\pi^{1/2}(\tilde{\gamma}_{13}\bar{\Gamma}/ku\gamma_2)(1-r^2)^{-1/2},$$

so that the SW chain contribution will dominate at high pressures, $\tilde{\gamma}_{13}/\gamma_2\gg 1$. The fact that the

first two terms have their maxima at different positions will lead to an asymmetric profile even if there are no velocity-changing collisions ($r = 1$). The third term will enhance the asymmetry, since its maximum position is far removed from the first two (assuming $\Delta_{21} \neq 0$).

These general line-shape features are illustrated in Fig. 4 for a detuning $\Delta_{21} = -0.5ku$ and the same collision parameters used in Fig. 3. A velocity-changing collision rate $\Gamma(2) = 2\gamma_2$ ($\alpha = \frac{1}{3}$) has been chosen and the three curves correspond to $\beta = 0$ (strong collisions), $\beta = 0.8$ (moderate collisions), and $\beta = 1$ (no velocity-changing collisions). As predicted, the curves are asymmetric, with the effects of velocity-changing collisions clearly evident in the broad shoulders of the $\beta = 0$ and $\beta = 0.8$ curves. The resonance near $\tilde{\Delta}_{23} = -\tilde{\Delta}_{21}$ is broader for the $\beta = 1$ case than the others; for $\beta = 1$, $\alpha = 1$ from Eq. (53) and the resonance is dominated by the second term in Eq. (54), which has a HWHM of $\bar{\Gamma} = \tilde{\gamma}_{12} + \tilde{\gamma}_{23}$, rather than by the first term in Eq. (54), which has a HWHM $\approx \tilde{\gamma}_{13} < \bar{\Gamma}$. At higher perturber pressures, α will decrease and the velocity-changing term in Eq. (54) will become dominant, reflecting the fact that at high pressures it becomes extremely likely for atoms in state 2 to collide before being excited to state 3.

Figure 4 is graphic proof that collisions can help distinguish the TQ and SW chains. Experimental verification of such curves would provide new insight into the nature of velocity-changing collisions. It should be noted that some offset of the laser $\Delta_{21} \neq 0$ is recommended to enhance the visibility of the velocity-changing effects. If $\Delta_{21} = 0$ is taken, all contributions to the line shape will be centered at approximately the same frequency.

B. Degeneracy

When level degeneracy is taken into account, the line-shape formulas become expectedly more complex. The degeneracy of levels 1 and 3 does not add any major complication. In fact, the TQ chain may be calculated with little modification [the Lorentzians which appear in Eq. (41a) may be replaced by sums of Lorentzians]. However, it is no easy matter to include collisional changes in level-2 density matrix elements $\rho_{2m;2m'}(\vec{v})$. The general propagator $G^{rh}_{pq}(\vec{v} \to \vec{v}', 2)$ determines the magnetic reorientation, phase, and velocity-changing effects occurring in collisions between atoms in level 2 and perturber atoms. Methods for approximating or modeling the propagator are not obvious. Some general symmetry arguments may be used to reduce the number of independent elements $G^{rh}_{pq}(\vec{v} - \vec{v}'; 2)$, and in the extreme case of fast isotropic perturbers there are but two nonzero independent elements.[26] On the other hand, there are cases where degeneracy can actually simplify matters. A specific case of this type is discussed in Sec. VI, where it will be shown that the level-2 degeneracy may be exploited to provide a sharper picture of velocity-changing collisions than can be seen in Fig. 4 of the nondegenerate case.

VI. LINE SHAPE—$J = 0 \to 1 \to 0$

In order to study velocity-changing collisions, it would be desirable to isolate the third term in Eq. (54), since this term contains all the velocity-changing effects. However, in the nondegenerate case, such an isolation is not possible, and the resultant line shape (Fig. 4) contains contributions from atoms which have not undergone velocity-changing collisions as well as from those which have had their velocity changed while in level 2. One can achieve the desired isolation if he is willing to consider degenerate systems. As a specific example, level 1 is taken to have $J = 0$, level 2 to have $J = 1$, and level 3 to have $J = 0$. Furthermore, the field $\vec{E}_1$ is chosen to be left-hand circularly polarized (LCP), $\vec{E}_2$ to be right-hand circularly polarized (RCP), and the two fields to propogate in opposite directions $\hat{k}_2 = -\hat{k}_1$.

Since $\vec{E}_1$ and $\vec{E}_2$ can each only induce $\Delta m = 1$ transitions (the z axis of quantization has arbitrarily been fixed parallel to $\vec{k}_1$), there will be *no* excitation to level 3 in the absence of collisions. Hence the only way in which level 3 can become excited is if collisions reorient the atom when it is in level 2. Consequently, the total physical process involves an excitation of the $m = 1$ substate of level 2 by the field $\vec{E}_1$, a reorienting collision that changes the magnetic substate to $m = -1$ accompanied by some change in velocity, and finally an excitation to level 3 by the field $\vec{E}_2$. The line shape arises solely from atoms which have undergone collisions while in level 2 and can serve as a direct monitor of velocity-changing collisions.

The mathematical treatment is straightforward. Using an orthogonal basis $(\hat{e}_1, \hat{e}_2, \hat{k}_1)$, one can determine that the complex amplitude $\vec{\mathcal{E}}_1$ for LCP light in Eq. (1a) is $\vec{\mathcal{E}}_1 = E_1(\hat{e}_1 + i\hat{e}_2)$ and the complex amplitude $\vec{\mathcal{E}}_2$ in Eq. (1b) for RCP light propagating in the $-\hat{k}_1$ direction is $\vec{\mathcal{E}}_2 = E_2(\hat{e}_1 + i\hat{e}_2)$. The corresponding field-strength quantities χ appearing in Eqs. (17) may be easily evaluated, using the Wigner-Eckart theorem, as

$$\chi^{(1)}_{2p;10} = -(\sqrt{2}\, eT_{21}E_1/\hbar)\delta_{p,1}\,, \tag{55a}$$

$$\chi^{(2)}_{30;2p} = -[(2/3)^{1/2} eT_{32}\, E_2/\hbar]\,\delta_{p,-1}\,, \tag{55b}$$

where T_{21} and T_{32} are reduced matrix elements of $\vec{r}$ between states 2 and 1 and states 3 and 2, respectively. With this result, the necessary products of χ's needed in Eqs. (32) are

$$A^{hjqh}_{sjqs}=0,$$
$$A^{hjqr}_{sjqp}=\tfrac{4}{3}\,|eT_{21}T_{32}E_1E_2/\hbar|^2\delta_{s,1}\delta_{h,1}\delta_{r,-1}\delta_{p,-1} \quad \text{(no sum)}. \tag{56}$$

Since A^{hjqh}_{sjqs} appears in the TQ expression (32a), two-quantum processes will not contribute to the line shape. This result is a direct consequence of our state-dependent collision model in which it is impossible for collisions to change the magnetic quantum numbers associated with off-diagonal density matrix elements of the form $\rho_{\alpha m:\alpha' m'}$ for $\alpha\neq\alpha'$ [see also Eq. (30a)]. Should line shapes exhibit structure characteristic of TQ processes (narrow resonance centered at $\tilde{\Delta}_{31}=0$) one would be forced to reassess the collision model for that particular case.

Thus the line shape arises solely from the SW term (32b) which, for the $J=0\to1\to0$ cascade, reduces to

$$I=4N_0(\gamma_3)^{-1}A'\,\tilde{\gamma}_{10:21}\tilde{\gamma}_{2-1:30}\times\int d^3v\int d^3v_0\,\mathfrak{L}^{ph}_{2-1:30}(\vec{v})G^{11}_{-1-1}(\vec{v}_0\to\vec{v};2)\times\mathfrak{L}^{ph}_{10:21}(\vec{v}_0)W(\vec{v}_0)\,, \tag{57}$$

where $A'\equiv A^{100-1}_{100-1}$, and $\mathfrak{L}^{ph}_{\alpha m:\alpha' m'}(\vec{v})$ and $\tilde{\gamma}_{\alpha m:\alpha' m'}$ are obtained from obvious generalizations of Eqs. (37), (38), (42), and (43). Equation (57) has a Lorentzian $\mathfrak{L}^{ph}_{10:31}(\vec{v}_0)$ representing an absorption to substate $m=1$ of level 2, a propagator $G^{11}_{-1-1}(\vec{v}_0\to\vec{v};2)$ representing the collisional transfer from $m=1$ to $m=-1$ accompanied by a change in velocity from $\vec{v}_0$ to $\vec{v}$, and a Lorentzian $\mathfrak{L}^{ph}_{2-1:30}(\vec{v})$ representing an absorption from substate $m=-1$ of level 2 to level 3. To determine the propagator, one must solve the coupled set of equations (35). However, in the spirit of Sec. V we choose instead a phenomenological propagator

$$G^{11}_{-1-1}(\vec{v}_0\to\vec{v};2)=(\gamma_2)^{-1}P_{-11}(\alpha)[\pi(1-r^2)u^2]^{-3/2}\times\exp[-(\vec{v}-r\vec{v}_0)/(1-r^2)u^2], \tag{58}$$

where r and α are defined as before [Eqs. (44b) and (45), respectively] and $P_{-11}(\alpha)$ is the steady-state relative probability of finding an atom in substate $m=-1$ when atoms are produced in state $m=1$. At low pressures ($\alpha\approx1$), $P_{-11}\sim1-\alpha$, since in the limit of no collisions P_{-11} must vanish. On the other hand, at higher pressures ($\alpha\approx0$), $P_{-11}\sim\frac{1}{3}$, since collisions will have caused total relaxation of the magnetic substate population. A reasonable form for P_{-11} is then

$$P_{-11}(\alpha)=(1-\alpha)/[1+2(1-\alpha)]\,. \tag{59}$$

Admittedly, the propagator (58) is oversimplified. A somewhat more realistic propagator would contain several parameters $\alpha_{mm'}$, reflecting the fact that collision rates depend on the magnetic quantum numbers involved. Correspondingly, the function P_{-11} would take on a different form,[27] as would the other factors in Eq. (58).

Substituting Eq. (58) into (57) and performing the indicated integrations, one obtains the line shape for the region of interest $|\Delta_{21}|<ku$ as

$$I=\frac{4\pi^{1/2}N_0A'P_{-11}(\alpha)}{k_1u\gamma_2\gamma_3}\exp\left[-\left(\frac{\Delta_{21}+\delta^{ph}_{10:21}}{ku}\right)^2\right]\times\frac{\bar{\Gamma}'}{(\bar{\Gamma}')^2+(\bar{\Delta}')^2},\quad\text{for }\beta\approx1; \tag{60a}$$

otherwise

$$I=\frac{4\pi N_0A'P_{-11}(\alpha)}{k_1k_2u^2\gamma_2\gamma_3(1-r^2)^{1/2}}\exp\left[-\left(\frac{\Delta_{21}+\delta^{ph}_{10:21}}{k_1u}\right)^2\right]\times\exp\left(-\frac{[\Delta_{32}+\delta^{ph}_{2-1:30}+(k_2/k_1)r(\Delta_{21}+\delta^{ph}_{10:21})]^2}{(k_2u)^2(1-r^2)}\right), \tag{60b}$$

where

$$\bar{\Gamma}'=\tilde{\gamma}_{2-1:30}+(k_2/k_1)\tilde{\gamma}_{10:21},\quad\bar{\Delta}'=\tilde{\Delta}_{30:2-1}+(k_2/k_1)\tilde{\Delta}_{21:10}, \tag{61}$$

and the Doppler limit (47) has been assumed but condition (3) has *not* been invoked. For weak collisions ($\beta\approx1$) and nonexcessive pressures ($\alpha\neq0$, implying $r=\beta^{1/\alpha}\approx1$), collisions do not significantly alter the atomic velocity and, as expressed in Eq. (60a), the line shape is Lorentzian, centered at

$$\Delta_{32}=-\delta^{ph}_{2-1:30}-(k_2/k_1)(\Delta_{21}+\delta^{ph}_{10:21}),$$

with HWHM of $\bar{\Gamma}'$. For somewhat stronger collisions, $(1-\beta^2)^{1/2}ku\gg\tilde{\gamma}_{\alpha m:\alpha' m'}$, the line shape reflects the velocity-changing collisions and is a Gaussian centered at

$$\Delta_{32}=-\delta^{ph}_{2-1:30}-(k_2/k_1)r(\Delta_{21}+\delta^{ph}_{10:21})$$

with width $k_2u(1-r^2)^{1/2}$. The above features are seen in Fig. 5, which is drawn using $k_1=k_2$ and the same parameters as in Fig. 4. The background of the TQ and no-collision SW processes have been eliminated, and the resulting line shape clearly illustrates the effects of velocity-changing collisions. At a given pressure, the shift of the line center from $-\tilde{\Delta}_{21}$ is a measure of the strength of the velocity-changing collisions.

In Fig. 6, the amplitude factor $P_{-11}(\alpha)$, the shift of line center from $-\tilde{\Delta}_{21}$, and the width of the resonance is shown as a function of $1-\alpha$, assuming the

Doppler limit (47) and taking the collision-strength parameter $\beta = 0.8$. The quantity $1-\alpha$ varies with the collision rate $\Gamma(2)$ as $\Gamma(2)/[\gamma_2 + \Gamma(2)]$; at low pressures $1-\alpha \ll 1$ and at higher pressures $1-\alpha \approx 1$. As discussed above, the amplitude is proportional to the pressure at low pressures and saturates at higher pressures owing to the complete equalization of magnetic sublevels caused by collisions. The dimensionless shift $S = (\tilde{\Delta}_{32} + \tilde{\Delta}_{21})/\tilde{\Delta}_{21} = 1 - (k_2/k_1)r$ is a measure of the shift of the line center from $-\tilde{\Delta}_{21}$ owing to velocity-changing collisions. At low pressures, the shift provides a direct measure of the collision strength, since $r \approx \beta$; at higher pressures, $r \sim 0$, reflecting the fact that a sufficient number of collisions will cause a velocity thermalization of the sample, leading to a line centered at $\tilde{\Delta}_{32} \approx 0$. The width of the resonance is $(1-r^2)^{1/2} ku$, and is $(1-\beta^2)^{1/2} ku$ at low pressures and $\approx ku$ at higher pressures when complete velocity thermalization has occurred. At still higher pressures, where the Doppler limit is no longer valid, the line shape will become Lorentzian.

By studying at a given pressure line shapes of the type shown in Fig. 5 and by obtaining the pressure-dependent curves shown in Fig. 6, one can arrive at values for the collision parameters α, β, $\bar{\Gamma}$, $\mathcal{S}^{ph}_{10:21}$ and $\mathcal{S}^{ph}_{2-1:30}$. In this way, information on various collision cross sections as well as the collision-strength parameter β may be uncovered. There may be cases where the propagator (58) is not sufficient to explain certain experimental data. For example, if the collision

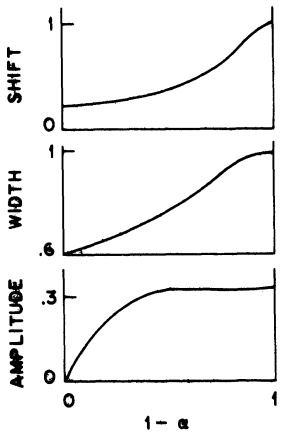

FIG. 6. Variation of the amplitude, shift, and width of the resonance shown in Fig. 5 as a function of pressure through the parameter $1-\alpha$. The curves are drawn for $\beta = 0.8$ but the general nature of the curves is independent of β. The shift shown is the dimensionless quantity $(\tilde{\Delta}_{32} + \tilde{\Delta}_{21})/\tilde{\Delta}_{21}$ evaluated at line center and is a measure of the line center's displacement owing to velocity-changing collisions. As shown, $k_1 = k_2$.

interaction has a long-range part plus a hard core, one may have to write the propagator as a sum of "weak-collision" and "strong-collision" parts. The line shape at moderate pressures $[(\beta_{\text{weak}})^{1/\alpha} \approx 1]$ would then consist of a Lorentzian plus a Gaussian. Rather than give results for many different propagators, we have concentrated on the simple propagators (44) and (58). As experimental data become available in the future, one may naturally seek to find propagators which give best fits to the data.

VII. EXTENSIONS OF THE THEORY

The theory outlined in the previous sections is a quite general one and can be extended to cover most cases of practical interest. Several possibilities for further investigation are listed below.

A. No Doppler cancellation

Although final expressions for the line shape have been given only for $|(\vec{k}_1 + \vec{k}_2)\cdot\vec{v}| \lesssim \gamma_{13}$ [with the exception of Eqs. (60)], the more general equations presented in this work are valid even if there is no Doppler cancellation and may be integrated without difficulty. The necessary modifications of the line-shape formulas under the conditions of no Doppler cancellation, $\hat{k}_2 = \epsilon \hat{k}_1$, $|k_1 - \epsilon k_2| u > \gamma_{13}$, are given in Appendix B, where $\epsilon = 1$ corresponds to copropagating and $\epsilon = -1$ to counterpropagating waves.

For counterpropagating waves, there is not much qualitative difference in the results. In the no-collision limit (analogous to Fig. 2), one must consider $|\Delta_{21}| \gg ku$ and $|\Delta_{21}| < ku$. If $|\Delta_{21}| \gg ku$, the line shape is a Gaussian with width $|k_2 - k_1| u$ centered at $\Delta_{31} = 0$; the Gaussian behavior is a direct consequence of the lack of Doppler cancellation. On the other hand, when $|\Delta_{21}| < ku$, only a small velocity subset of atoms effectively contributes to line-shape formation and the line is a Lorentzian centered at $\Delta_{32} = -(k_2/k_1)\Delta_{21}$ with a HWHM of $\frac{1}{2}[\gamma_3 + \gamma_2 |1 - (k_2/k_1)|]$. The HWHM is greater than the value of $\frac{1}{2}\gamma_3$ of the Doppler cancellation case. In the line shape corresponding to Fig. 3 (collisions with $|\Delta_{21}| \gg ku$), the resonance near $\Delta_{31} \approx 0$ will show a residual Doppler broadening, but the broad resonance at $\Delta_{32} \approx 0$ will be unchanged. The general nature of the curves corresponding to Figs. 4 and 5 will also remain unchanged, although the exact values of the widths and shifts will vary somewhat because of the introduction of new combinations of collisional widths and shifts in the line-shape formulas.

For copropagating waves, the line shape acquires a new and somewhat surprising feature.[15] If $|\Delta_{21}| < ku$, one can perform a contour integration of Eq.

(36a) in the Doppler limit [Eq. (47)] to show that $\tilde{\rho}_{33}^{TQ}=0$. The contributions from different velocity subsets of atoms leads to a cancellation of the $\tilde{\rho}_{33}^{TQ}$ contribution. Whether or not additional physical insight may be derived from this result remains to be seen. For copropagating waves, the line shapes corresponding to Figs. 2–4 would be changed as follows: Figure 2—if $|\Delta_{21}|\gg ku$ the resonance is a Gaussian with width $(k_1+k_2)u$ centered at $\Delta_{31}=0$, and if $|\Delta_{21}|<ku$ the resonance is a Lorentzian with HWHM of $\frac{1}{2}\{\gamma_3+\gamma_2[1+(k_2/k_1)]\}$ centered at $\Delta_{32}=-(k_2/k_1)\Delta_{21}$. Figure 3—the resonance at $\Delta_{31}\approx 0$ will be Doppler broadened, but the broad resonance at $\Delta_{32}\approx 0$ will be unchanged. Figure 4—the TQ contribution will be absent, but there will still be a narrow resonance arising solely from the SW chain given in Eq. (52).

B. Alternative level schemes

Instead of the upward cascade shown in Fig. 1, one could have equally well considered the up-down cascades shown in Fig. 7. The level scheme of Fig. 7(a) can be analyzed in a manner identical to that of the upward cascade with the substitution $\delta_{32}(\vec{v})\to -(\omega_{23}-\Omega_2+\vec{k}_2\cdot\vec{v})$, following Eqs. (16). The Doppler cancellation condition will now be possible only for copropagating waves, a well-known property in Raman scattering.

The level scheme of Fig. 7(b) provides three additional difficulties arising from the fact that level 1 and level 3 are now identical. First, a different collision model is required (see below). Second, each field can now drive *both* the upward and downward transitions leading to temporal population pulsations at the beat frequency [this would also be the case for Fig. 7(a) if the separation between levels 1 and 3 was small enough to invalidate Eqs. (2)]. Perturbation solutions are still possible, although a steady-state solution of the type posed in Eqs. (14) will now have to include time dependence in the populations. Finally, if level 1 is a ground state, one can no longer measure the final-state population through fluorescence. An alternative monitoring scheme is needed and might involve absorption measurements on the fields involved in the two-photon processes. It may be difficult to perform such absorption experiments at low enough field strengths for perturbation theory to be valid.

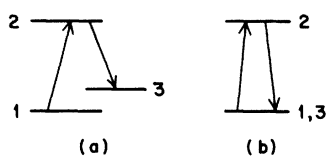

FIG. 7. Two alternative level schemes which may be used in collision studies.

C. Inelastic collisions

If any of the levels under consideration are part of a fine structure, hyperfine structure, or rotational energy multiplet, inelastic collisions may have to be taken into account. As long as collisions cannot couple any of the levels 1, 2, or 3, inelastic collisions can be included as additional decay or pumping parameters for each of the levels. If collisions can cause transitions between two of the levels [as would be the case in Fig. 7(a) if levels 1 and 3 were separated by less than thermal energy], a more detailed collision theory would have to be developed to consistently treat the collision-induced phase and velocity changes.

D. Different collision models

The collision model adopted in this work is appropriate to the case of levels 1, 2, and 3 experiencing significantly different collision interactions, as would normally occur if they were different electronic levels. However, if levels 1 and 3 in Fig. 7 belonged to the same electronic level, one might have adopted a model in which, to first approximation, collisions are velocity changing in their effect on $\tilde{\rho}_{13}(\vec{v})$. The $\tilde{\rho}_{13}(\vec{v})$ element appears only in the TQ chain; thus it is only that contribution which will be altered by the change in collision model. In the Doppler cancellation case, velocity-changing collisions play no role because of the cancellation of all velocity dependence in δ_{31}. Thus the line will be *narrower* than the corresponding case where phase-interrupting collisions broadened and shifted the TQ resonance. If there was no Doppler cancellation, the TQ resonance would have had some residual Doppler width. Velocity-changing collisions could narrow this width,[2-4,28] provided inelastic collisions did not mask the effect. As experiments provide further tests of the theory, one could abandon collision models altogether and attempt quantum-mechanical evaluation of the collision parameters given in Appendix A.

E. Resonant collisions

In order to analyze pumping schemes in gas lasers and the feasibility of laser isotope separation, it is necessary to determine the effects of collisions between similar atoms in addition to the effects of foreign-gas perturbers discussed in this work. The calculation will differ from the foreign-gas case only if level 2 is optically connected to the ground state. In that situation, the line shape will be affected by a resonant exchange of excita-

tion in a collision.[29] Diagonal density matrix elements (population) as well as off-diagonal density matrix elements (coherence) can be transferred in collisions.[30] Transfer of excitation will also imply a change in velocity, since the perturber which picks up the excitation has a velocity uncorrelated with that of the active atom. Thus in the SW chain, which is of primary interest for collision studies, the velocity distribution of those atoms excited by transfer will be Maxwellian, leading to an *additional* broad resonance centered about $\Delta_{32} = -S_{32}^{ph}$ in Fig. 5. Such results of resonant exchange are interesting and important enough to warrant further theoretical and experimental studies. One could reasonably hope to measure excitation transfer cross sections using these spectroscopic techniques.

F. Radiation trapping

At active-atom pressures, where resonant exchange is important ($\gtrsim 10$ mTorr), one usually encounters the added complication of radiation trapping. If level 1 is the ground state, then at pressures $\gtrsim 1.0$ mTorr any spontaneous emission from level 2 to level 1 will be absorbed by some other ground-state atom in the sample. Even if level 1 is not a ground state and provided there is a high enough pressure of active atoms, spontaneous radiation from any of the levels 1, 2, or 3 may be trapped if the levels are optically connected with the ground state. Radiation trapping has been considered by several authors.[31] Neglecting any collective affects, radiation trapping simply leads to a transfer of population and orientation from one level (1, 2, or 3) of an atom to the corresponding level of another atom, with no transfer of off-diagonal elements ($\rho_{\alpha m;\alpha' m'}, \alpha \neq \alpha'$).[32]

Radiation trapping on levels 1 and 3 would lead to an effective increase in their lifetime, but to no major influence on the line shape. However, in addition to an increased lifetime, trapping of radiation from level 2 can lead to a magnetic reorientation *plus* a velocity thermalization, since the velocity of the atom receiving the radiation is arbitrary. In this sense, radiation trapping produces the same effect as excitation transfer collisions or strong thermalizing collisions. It can be distinguished from these processes by its pressure dependence, however, since the contribution from radiation trapping will generally saturate at a pressure lower than that at which collision effects become important.

G. Strong fields

The calculation may be generalized[14-17,20,33] to treat cases where the fields $\vec{E}_1$, $\vec{E}_2$, or both are strong enough so that perturbation theory is no longer applicable. Analytic solutions are possible only for oversimplified collision models, but some physical insight is still obtainable with these models. For the strong-field case, it becomes difficult to easily extract velocity-changing effects from the line shapes owing to complications of power broadening. It seems highly appropriate to conduct weak-field experiments if the major goal is to obtain information on collision mechanisms.

VIII. EXPERIMENTAL CONSIDERATIONS

There are several methods which can be used for experimental studies of collision effects. Laser spectroscopic experiments which eliminate Doppler broadening generally can be characterized as either fluorescence or absorption measurements. In fluorescence experiments, a laser is used to drive a given transition, and one measures the fluorescence spectrum or total fluorescence from a coupled transition. For the calculation outlined in this paper, the level-3 fluorescence as a function of Δ_{32} provides the necessary line shape for collisional studies. Fluorescence experiments have the major advantage of a high detection efficiency, enabling one to use laser light of sufficiently low intensity to avoid power broadening. On the other hand, in absorption measurements, one generally saturates a given transition with a pump beam and monitors the absorption of a probe beam on the same or a coupled transition. Power broadening does play a role in these experiments and results must be extrapolated to zero pump intensity. Both fluorescence and absorption experiments can provide data on collision cross sections and the strength of velocity-changing collisions.

For the two-photon excitation line profiles discussed in this work, the HWHM in the absence of collisions is $\frac{1}{2}\gamma_3$, if the Doppler cancellation condition (3) is appropriate, or $\frac{1}{2}(\gamma_3 + \gamma_2 |1 - k_2/k_1|)$, if that condition is not met but the tuning is such that $|\Delta_{21}| < ku$. Thus it is clear that for high-resolution spectroscopy the sharpest lines are obtainable in the Doppler cancellation regime. However, as long as $|\Delta_{21}| < ku$, the no-collision line shape is still much narrower than the Doppler width. With regard to collision studies, it is really unimportant whether or not Eq. (3) is valid, since the overall qualitative nature of the results is not affected severely. In fact, by using copropagating waves in the upward cascade for $|\Delta_{21}| < ku$, the line shape is simplified by the absence altogether of the TQ contribution, although this is at the expense of a somewhat larger no-collision HWHM of $\frac{1}{2}[\gamma_3 + \gamma_2(1 + k_2/k_1)]$.

The major advantage of using applied fields with propagation vectors $\vec{k}_1$ and $\vec{k}_2$ such that $|\vec{k}_1+\vec{k}_2|u<\gamma_{13}$ is that for $|\Delta_{21}|\gg ku$ narrow resonances may be obtained about $\Delta_{31}=0$. One way to insure this Doppler cancellation condition is to use counterpropagating waves of the *same* frequency $\vec{k}_1=-\vec{k}_2$, as has been done by several groups.[12] In that case, the two-photon resonance occurs at $k_1c=\Omega_1=\frac{1}{2}(\omega_{21}+\omega_{32})$, with width γ_{13}. However, since one cannot tune Ω_2 and Ω_1 separately, this technique is not ideally suited for comprehensive collision studies, but it may be used solely to determine Γ_{13}^{ph} and $\mathcal{S}_{13}^{ph}$. Moreover, if $\frac{1}{2}(\omega_{21}+\omega_{32})-\omega_{21}\gg ku$, the signal strength is such experiments will be down significantly owing to a lack of resonant enhancement from the intermediate state. The $3S\rightarrow 3P\rightarrow 5S$ transition in Na provides an example where the Doppler cancellation condition can be maintained for $|\Delta_{21}|\gg ku$, without sacrificing any substantial loss in resonant enhancement [even when $\Delta_{21}\approx 0$, the Doppler cancellation condition is approximately satisfied, since $(\omega_{21}-\omega_{32})u/c\approx 10^8$ sec^{-1}, while $\gamma_{13}\approx 10^7$ sec^{-1}].

It should be stressed that studies of velocity-changing collisions require $|\Delta_{21}|<ku$; whether or not the Doppler cancellation condition can be maintained in this tuning range is really of little importance and should not influence the choice of transition scheme to be studied.

While there have not been experimental investigations carried our precisely along the lines discussed in this work, there have been related studies, several of which are listed below:

Bishel *et al.*[10] performed an upward-cascade absorption measurement on vibrational transitions in CH_3F and investigated the narrow resonance shown in Fig. 3, $|\Delta_{21}|\gg ku$. They determined the broadening and shift of this resonance as a function of pressure. The existence of a shift of 2.1 MHz/Torr for CH_3F perturbers implies that the collisional interaction for the (0, 1, 1) and (2, 3, 1) vibrational levels of CH_3F differ somewhat. The large broadening coefficient of 41 MHz/Torr they found is due mainly to inelastic collisions.

Rousseau *et al.*[11] measured the forward Raman scattering of I_2 with I_2 perturbers for the case $|\Delta_{21}|>ku$. Their work verifies the existence of the entire line shape shown in Fig. 3, although it appears that they fit the broad resonance to a Lorentzian rather than a Gaussian shape.

Beterov *et al.*[9] probed the $2s_2$-$2p_4$ transition in Ne with a strong field applied to the coupled $2s_2$-$2p_1$ transition. The perturbers were Ne, and absorption for both copropagating and counterpropagating probe beams were monitored for $\Delta_{21}=0$. Curves similar to those in Fig. 4 were obtained with a broad Gaussian background which was attributed to radiation trapping and resonance exchange effects (see discussion of Sec. VII). By measuring absorption widths for both copropagating and counterpropagating waves, various collision rates and cross sections were determined. Further information on the collision interaction could have been obtained had they detuned the pump laser so that $\Delta_{21}\neq 0$. In that case, it would have been easier to uncover the existence of elastic nonexcitation transfer collisions which give rise to line shapes of the type shown in Fig. 4.

Smith and Hänsch[7] performed a saturated absorption experiment on the 6328-Å line in Ne and also obtained the broad Gaussian background, presumably due to radiation trapping or excitation transfer from the $3s_2$ level.

Hänsch and Toschek[6] and Keil *et al.*[8] did saturation spectroscopy on Ne, but took a case where $2p_4$ rather than $3s_2$ was the level common to both transitions. In this manner, radiation trapping and excitation transfer effects no longer significantly influence the line shape. The pump light was tuned to resonance, $\Delta_{21}=0$, and depolarizing collisions were monitored for both He and Ne perturbers. The experimental results indicate that the average velocity change per collision is small, $\Delta v/v<0.01$, and as might have been expected is larger for neon than for helium perturbers. The line shape remains close to Lorentzian, supporting a weak-collision model. The experiments also tend to validate the line shapes of Fig. 5 in that all magnetic substate changing collisions were accompanied by a change in velocity.

The above choice of experiments is meant to be representative rather than complete. There seems to be growing evidence that velocity-changing collisions in gases are characterized by small changes in velocity. Recent experiments on inelastic collisions in[34] CO_2 and[35] CH_3F and elastic collisions in[36] CH_3F have lent support to this hypothesis.[37] A photon-echo experiment[36] on a vibrational transition in CH_3F led to the conclusion that the collision interaction for the two levels involved was the same, at least to first order. Many additional experiments are needed to systematically analyze collisional processes in atomic and molecular systems.

IX. CONCLUSIONS

A theoretical discussion of collision effects in two-photon spectroscopy has been presented. Two-photon spectroscopy offers unique possibilities for collision studies. Collisional dephasing rates, excitation transfer cross sections, state-dependent collision rates, magnetic relaxation rates, and average changes in velocity per collision can be extracted from the line shapes. Moreover, the line

shapes may provide fundamental tests of recent collision theories[2-4] that purport to consistently treat both phase-changing and velocity-changing collisions. The most conclusive verification of these quantum-mechanical collision-broadening theories would involve experiments on transitions between states experiencing somewhat different collision interactions. According to theory, there will be velocity-changing effects associated with diagonal density matrix elements, but phase-changing effects associated *only* with off-diagonal density matrix elements.

A general formalism was given to account for binary collision effects within the impact approximation. The specific calculation involved two-photon excitation in a three-level upward cascade. This system may prove especially useful for studying resonant collision effects involving the intermediate and ground states. Since the radiation between those states will be almost completely trapped at typical experimental pressures, the resonant processes must be monitored on some other transition. In the two-photon scheme of Fig. 1, fluorescence from level 3 will serve as an indirect measure of resonant collision processes involving the 1-2 transition.

It is hoped that additional experiments will be carried out to provide new inputs for the theory. From a theoretical point of view, the easiest experiments to analyze would involve transitions between nondegenerate levels in systems subjected to foreign-gas broadening at low pressures and low laser powers. Studies of line shapes versus pressure for a fixed detuning $\Delta_{21} \neq 0$ of one of the lasers could yield important information on collision mechanisms in atomic and molecular systems.

ACKNOWLEDGMENTS

I am pleased to acknowledge stimulating discussions with Dr. P. Liao and J. Lam.

APPENDIX A

This Appendix is divided into two parts. In the first part, a formal solution for the two-photon excitation rate in the presence of collisions is developed. In the second part, a collision model is assumed and the formal results are seen to reduce to Eqs. (30) and (32) of the text.

Formal solution

Assuming that collisions with nondegenerate ground-state perturbers cannot induce transitions between active-atom states 1, 2, and 3 of Fig. 1 but can induce transitions among the sublevels of any individual state, a general form for the collisional time rate of change of density matrix elements is

$$\frac{\partial \tilde{\rho}_{\alpha m;\alpha' m'}(\vec{v},t)}{\partial t} = \int d^3v' S^{\alpha n;\alpha' n'}_{\alpha m;\alpha' m'}(\vec{v}'\to\vec{v})\tilde{\rho}_{\alpha n;\alpha' n'}(\vec{v}',t), \quad \text{(A1)}$$

where

$$S^{\alpha n;\alpha' n'}_{\alpha m;\alpha' m'}(\vec{v}'\to\vec{v}) = R^{\alpha n;\alpha' n'}_{\alpha m;\alpha' m'}(\vec{v})\delta(\vec{v}'-\vec{v}) + W^{\alpha n;\alpha' n'}_{\alpha m;\alpha' m'}(\vec{v}'\to\vec{v}), \quad \text{(A2)}$$

$$R^{\alpha n;\alpha' n'}_{\alpha m;\alpha' m'}(\vec{v}) = -N\int d^3v_p W_p(\vec{v}_p) v_r \left(\frac{2\pi\hbar}{i\mu v_r}[f_{mn}(\vec{v}_r\to\vec{v}_r;\alpha)\delta_{m',n'} - f_{m'n'}(v_r\to v_r;\alpha')^*\delta_{m,n}]\right), \quad \text{(A3)}$$

$$W^{\alpha n;\alpha' n'}_{\alpha m;\alpha' m'}(\vec{v}'\to\vec{v}) = N\left(\frac{m}{\mu}\right)^3 \int d^3v_p' \int d^3v_r W_p(\vec{v}_p') v_r^{-1}\, \delta\left(\vec{v}_r + \frac{m}{m_p}\vec{v}' - \frac{m}{\mu}\vec{v} + \vec{v}_p'\right)\delta(v_r - v_r') \times f_{mn}(\vec{v}_r'\to\vec{v}_r;\alpha) f_{m'n'}(\vec{v}_r'\to\vec{v}_r;\alpha')^*, \quad \text{(A4)}$$

and where N is the perturber density, $W_p(\vec{v}_p)$ is the perturber velocity distribution, $\vec{v}_r = \vec{v} - \vec{v}_p$ and μ are the active-atom–perturber relative velocity and reduced mass, respectively, $f_{mn}(\vec{v}_r'\to\vec{v}_r;\alpha)$ is the inelastic scattering amplitude for scattering from state $|\alpha m\rangle$ with velocity $\vec{v}_r'$ to state $|\alpha n\rangle$ with velocity $\vec{v}_r = \hat{v}_r v_r'$, $\vec{v}_r' = \vec{v}' - \vec{v}_p'$, m and m_p are the active-atom and perturber masses, and the implicit sum in Eq. (A1) is over repeated *latin* indices. Equations (A3) and (A4) are analyzed in detail elsewhere[4] and will be examined below for a specific collision model. However, for the present, Eq. (A1) will be discussed.

The right-hand side of Eq. (A1) is added to the rhs of Eqs. (16) to obtain equations for steady-state density matrix elements in the presence of collisions. Each of the equations (16) takes the form

$$\eta_{\alpha\alpha'}(\vec{v})\tilde{\rho}_{\alpha m;\alpha' m'}(\vec{v}) = \int d^3v' S^{\alpha n;\alpha' n'}_{\alpha m;\alpha' m'}(\vec{v}'\to\vec{v})\tilde{\rho}_{\alpha n;\alpha' n'}(\vec{v}') + g_{\alpha m;\alpha' m'}(\vec{v}), \quad \text{(A5)}$$

where

$$\eta_{\alpha\alpha'}(\vec{v}) = \gamma_{\alpha\alpha'} - i\delta_{\alpha'\alpha}(\vec{v}) \tag{A6}$$

and $g_{\alpha m:\alpha' m'}(\vec{v})$ is the rhs of the corresponding $\tilde{\rho}_{\alpha m:\alpha' m'}(\vec{v})$ equation; for example,

$$g_{1m:3m'}(\vec{v}) = i\chi^{(1)*}_{2p:1m}\tilde{\rho}_{2p:3m'}(\vec{v}) - i\chi^{(2)*}_{3m':2p}\tilde{\rho}_{1m:2p}(\vec{v}) .$$

To obtain a formal solution to Eq. (A5) that is well suited for perturbation calculations, one can introduce propagators $G^{\alpha n:\alpha' n'}_{\alpha m:\alpha' m'}(\vec{v}' \to \vec{v})$ through the equation[4,38]

$$\tilde{\rho}_{\alpha m:\alpha' m'}(\vec{v}) = \int d^3v' G^{\alpha n:\alpha' n'}_{\alpha m:\alpha' m'}(\vec{v}' \to \vec{v}) g_{\alpha n:\alpha' n'}(\vec{v}') , \tag{A7}$$

where the propagators will now contain all collisional information and obey the coupled equations

$$\eta_{\alpha\alpha'}(\vec{v}) G^{\alpha n:\alpha' n'}_{\alpha m:\alpha' m'}(\vec{v}' \to \vec{v}) = \delta(\vec{v} - \vec{v}')\delta_{m,n}\delta_{m',n'} + \int d^3v_1 S^{\alpha q:\alpha' q'}_{\alpha m:\alpha' m'}(\vec{v}_1 \to \vec{v}) G^{\alpha n:\alpha' n'}_{\alpha q:\alpha' q'}(\vec{v}' \to \vec{v}_1) . \tag{A8}$$

Equation (A5) may be solved by a straightforward iterative perturbative technique [recall that g is just the rhs of Eqs. (16)]. The lowest-order term in the calculation follows from Eqs. (16a), (A5), and (A6) as

$$\tilde{\rho}^{(0)}_{1m:1m'}(\vec{v}) = \int d^3v' G^{1n:1n'}_{1m:1m'}(\vec{v}' \to \vec{v}) \lambda(\vec{v}')\delta_{n,n'} . \tag{A9}$$

If the pumping rate $\lambda(\vec{v})$, as defined by Eq. (25), represents an equilibrium velocity distribution and if, as assumed, all sublevels are equally pumped, collisions can have no effect on the velocity distribution and

$$\rho^{(0)}_{1m:1m'}(\vec{v}) = [\lambda(\vec{v})/\gamma_1]\delta_{m,m'} , \tag{A10}$$

as in the no-collision case. Higher-order terms may be calculated from Eqs. (16) and (A5) for the two perturbative chains depicted in expression (19). The TQ and SW contributions to the line shape

$$I_{mm'} = \int d^3v \, [\tilde{\rho}^{TQ}_{3m:3m'}(\vec{v}) + \tilde{\rho}^{SW}_{3m:3m'}(\vec{v})] \equiv \rho^{TQ}_{3m:3m'} + \rho^{SW}_{3m:3m'} \tag{A11}$$

are

$$\rho^{TQ}_{3m:3m'} = N_0 A^{hjfn}_{srqp} \int d^3v d^3v_3 d^3v_2 d^3v_1 d^3v_0 W(\vec{v}_0) \times [G^{3q:3q'}_{3m:3m'}(\vec{v}_3 \to \vec{v}) G^{2s:3t}_{2p:3q'}(\vec{v}_2 \to \vec{v}_3) G^{1w:3f}_{1r:3t}(\vec{v}_1 \to \vec{v}_2) G^{1j:2h}_{1w:2n}(\vec{v}_0 \to \vec{v}_1) + G^{3q':3f}_{3m:3m'}(\vec{v}_3 \to \vec{v}) G^{2h:3t}_{2n:3q'}(\vec{v}_2 \to \vec{v}_3)^* G^{1w:3q}_{1j:3t}(\vec{v}_1 \to \vec{v}_2)^* G^{1r:2s}_{1w:2p}(\vec{v}_0 \to \vec{v}_1)] , \tag{A11a}$$

$$\rho^{SW}_{3m:3m'} = N_0 A^{hjtr}_{snqp} \int d^3v d^3v_3 d^3v_2 d^3v_1 d^3v_0 W(\vec{v}_0) \times \{ G^{3q:3q'}_{3m:3m'}(\vec{v}_3 \to \vec{v}) G^{2g:3t}_{2p:3q'}(\vec{v}_2 \to \vec{v}_3) [G^{2s:2f}_{2g:2r}(\vec{v}_1 \to \vec{v}_2) G^{1j:2h}_{1n:2f}(\vec{v}_0 \to \vec{v}_1) + G^{2f:2h}_{2g:2r}(\vec{v}_1 \to \vec{v}_2) G^{1n:2s}_{1j:2f}(\vec{v}_0 \to \vec{v}_1)^*] + G^{3q':3t}_{3m:3m'}(\vec{v}_3 \to \vec{v}) G^{2g:3q}_{2r:3q'}(\vec{v}_2 \to \vec{v}_3)^* [G^{2s:2f}_{2p:2g}(\vec{v}_1 \to \vec{v}_2) G^{1j:2h}_{1n:2f}(\vec{v}_0 \to \vec{v}_1) + G^{2f:2h}_{2p:2g}(\vec{v}_1 \to \vec{v}_2) G^{1n:2s}_{1j:2f}(\vec{v}_0 \to \vec{v}_1)^*] \} , \tag{A11b}$$

where $N_0 = \lambda/\gamma_1$ and A is defined by Eq. (33). Equations (A11), together with Eqs. (A8), represent a formal solution to the problem.

Collision model

The collision model to be adopted is based on the assumption that the scattering for the electronic atomic states 1, 2, and 3 is strongly state dependent. Consequently, the overlap term in Eq. (A4) is assumed to vanish, owing to interference effects, unless $\alpha = \alpha'$. There may be some nonzero contribution from Eq. (A4) for small-angle scattering even if $\alpha \neq \alpha'$, but this contribution is taken to be negligible in comparison with that from Eq. (A3). In this model, all collision kernels with $\alpha \neq \alpha'$ are zero, and the diagonal terms are written in a slightly different notation as

$$W^{\alpha n:\alpha' n'}_{\alpha m:\alpha' m'}(\vec{v}' \to \vec{v}) = W^{nn'}_{mm'}(\vec{v}' \to \vec{v};\, \alpha)\, \delta_{\alpha,\alpha'} . \tag{A12}$$

The kernel $W^{nn'}_{mm'}(\vec{v}' \to \vec{v}; \alpha)$ appears in Eqs. (30b) and (35) of the text. Equation (A12) reflects the basic feature of the model; collisions cannot change the velocity associated with off-state ($\alpha \neq \alpha'$) density matrix elements $\tilde{\rho}_{\alpha m:\alpha' m'}(\vec{v})$. For state-independent collision interactions, the model will no longer be valid.

One further simplification is possible before proceeding to the final line-shape formula. Regardless of the collision model, the forward inelastic scattering amplitudes in Eq. (A3) will vanish, since the internal atomic angular momentum cannot be changed in collisions that involve no change in the velocity of the atoms. One may then rewrite Eq. (A3) in such a way as to define the parameters $\gamma^{ph}_{\alpha m:\alpha' m'}$ and $R^{nn}_{mm'}(\vec{v};\alpha)$ appearing in the text, taking

$$R^{\alpha n:\alpha' n'}_{\alpha m:\alpha' m'}(\vec{v}) = -\gamma^{ph}_{\alpha m:\alpha' m'}(\vec{v})\delta_{m,n}\delta_{m',n'}, \tag{A13}$$

for $\alpha \neq \alpha'$, and

$$R^{\alpha n:\alpha' n'}_{\alpha m:\alpha' m'}(\vec{v}) = -R^{nn'}_{mm'}(\vec{v};\alpha), \tag{A14}$$

for $\alpha = \alpha'$. The forward elastic scattering amplitudes appearing in Eq. (A3) may be rewritten in terms of cross sections if one so desires.

Using Eq. (A12) and (A13) one may easily solve Eq. (A7) for the case $\alpha \neq \alpha'$, obtaining

$$G^{\alpha n:\alpha' n'}_{\alpha m:\alpha' m'}(\vec{v}' \to \vec{v}) = \mathfrak{D}_{\alpha m:\alpha' m'}(\vec{v})\delta(\vec{v}-\vec{v}')\delta_{m,n}\delta_{m',n'}, \tag{A15}$$

where

$$\mathfrak{D}_{\alpha m:\alpha' m'}(\vec{v}) = [\eta_{\alpha\alpha'}(\vec{v}) + \gamma_{\alpha m:\alpha' m'}(\vec{v})]^{-1} \tag{A16}$$

appears in Eq. (34) [in Eq. (34), the $\vec{k}$ dependence of $\eta_{\alpha\alpha'}(\vec{v})$ is explicitly noted]. Using this result and the notation of Eqs. (A12) and (A14), one can reduce Eqs. (A11) to the form

$$\rho^{TQ}_{3m:3m'} = N_0 A^{hjfh}_{sjqs}\int d^3v\, d^3v_0\, W(\vec{v}_0)G^{qf}_{mm'}(\vec{v}_0\to\vec{v};3)[\mathfrak{D}_{2s:3f}(\vec{v}_0)\mathfrak{D}_{1j:3f}(\vec{v}_0)\mathfrak{D}_{1j:2h}(\vec{v}_0) + \mathfrak{D}_{2h:3q}(\vec{v}_0)^*\mathfrak{D}_{1j:3q}(\vec{v}_0)^*\mathfrak{D}_{1j:2s}(\vec{v}_0)^*], \tag{A17a}$$

$$\rho^{SW}_{3m:3m'} = N_0 A^{hjtr}_{sjqp}\int d^3v\, d^3v_2\, d^3v_0\, W(\vec{v}_0)G^{qt}_{mm'}(\vec{v}_2\to\vec{v};3)[\mathfrak{D}_{2p:3t}(\vec{v}_2) + \mathfrak{D}_{2r:3q}(\vec{v}_2)^*]G^{sh}_{pr}(\vec{v}_0\to\vec{v}_2;2)[\mathfrak{D}_{1j:2h}(\vec{v}_0) + \mathfrak{D}_{1j:2s}(\vec{v}_0)^*]. \tag{A17b}$$

If there is interest only in the excited-state population, one should set $m' = m$ in Eqs. (17). Setting $m' = m$ and using the fact, easily derived from Eq. (A7), that

$$\int G^{qt}_{mm}(\vec{v}'\to\vec{v};\alpha)\, d^3v = (\gamma_\alpha)^{-1}\delta_{q,t}, \tag{A18}$$

one arrives at Eqs. (32) of the text.

APPENDIX B

If one takes $\hat{k}_2 = \epsilon\hat{k}_1$ and $|k_1 - \epsilon k_2| > \gamma_{13}$, the Doppler cancellation line shapes are no longer applicable. However, the more general expressions in the text are easily integrated over velocity even when Eq. (3) is not valid. The necessary modifications of the line shape for the two cases $\epsilon = 1$ (copropagating) and $\epsilon = -1$ (counterpropagating) are as follows:

(a) Equations (29) become

$$I_{mm'} = \frac{2\pi^{1/2}N_0 A_{mm'}e^{-(\Delta_{21})^2/k_1^2u^2}}{k_1 u\gamma_3\gamma_2} \times \frac{\gamma_3 + \frac{1}{2}\gamma_2|1+\epsilon k_2/k_1|}{(\gamma_3+\frac{1}{2}\gamma_2|1+\epsilon k_2/k_1|)^2 + (\Delta_{32} - \epsilon\Delta_{21}k_2/k_1)^2}, \quad |\Delta_{21}| < ku, \tag{B1a}$$

$$I_{mm'} = \frac{2\pi^{1/2}N_0 A_{mm'}}{(k_1+\epsilon k_2)u(\Delta_{21})^2\gamma_3}\exp\left[-\left(\frac{\Delta_{31}}{k_1+\epsilon k_2}\right)^2\right], \quad |\Delta_{21}| >> ku. \tag{B1b}$$

(b) Equation (49a) becomes the same as Eq. (B1b) with the substitution of $\bar{\Delta}_{31}$ for Δ_{31}. Equation (49b) is unchanged.

(c) Equation (51a) is replaced by

$$\rho^{TQ}_{33} = 0, \quad \text{for } \epsilon = 1, \tag{B2a}$$

$$\rho^{TQ}_{33} = 4\pi^{1/2}AN_0(\gamma_3)^{-1}\exp[-(\bar{\Delta}_{21})^2/(k_1u)^2] \times \begin{cases} \dfrac{k_2}{k_1-k_2}\dfrac{\bar{\Gamma}_1\bar{\Gamma}_2 - \bar{\Delta}_1\bar{\Delta}_2}{[(\bar{\Gamma}_1)^2+(\bar{\Delta}_1)^2][(\bar{\Gamma}_2)^2+(\bar{\Delta}_2)^2]}, & k_1 - k_2 > 0, \\ \dfrac{k_2}{k_2-k_1}\dfrac{\bar{\Gamma}_2\bar{\Gamma}_3 - \bar{\Delta}_2\bar{\Delta}_3}{[(\bar{\Gamma}_2)^2+(\bar{\Delta}_2)^2][(\bar{\Gamma}_3)^2+(\bar{\Delta}_3)^2]}, & k_2 - k_1 > 0, \end{cases} \tag{B2b}$$

for $\epsilon = -1$, where

$$\bar{\Gamma}_1 = \tilde{\gamma}_{23} + [k_2/(k_2 - k_1)]\,\tilde{\gamma}_{13}, \tag{B3a}$$

$$\bar{\Gamma}_2 = \tilde{\gamma}_{23} + (k_2/k_1)\tilde{\gamma}_{12}, \tag{B3b}$$

$$\bar{\Gamma}_3 = [k_2/(k_2 - k_1)]\,\tilde{\gamma}_{13} + (k_2/k_1)\tilde{\gamma}_{12}, \tag{B3c}$$

$$\bar{\Delta}_1 = \tilde{\Delta}_{32} + [k_2/(k_1 - k_2)]\,\tilde{\Delta}_{31}, \tag{B3d}$$

$$\bar{\Delta}_2 = \tilde{\Delta}_{32} + (k_2/k_1)\,\tilde{\Delta}_{21}, \tag{B3e}$$

$$\bar{\Delta}_3 = [k_2/(k_2 - k_1)]\,\tilde{\Delta}_{31} + (k_2/k_1)\tilde{\Delta}_{21}. \tag{B3f}$$

Equation (52) is modified simply by replacing $\bar{\Gamma}$ by $\bar{\Gamma}_2$ and $\bar{\Delta}$ by $\bar{\Delta}_2$. Equation (54) is then replaced by the sum of Eqs. (B2) and the modified Eq. (52).

(d) Equations (60) are unchanged.

---

*Supported by the U. S. Army Research Office.

[1]G. M. Carter, D. E. Pritchard, M. Kaplan, and T. W. Ducas, Phys. Rev. Lett. 35, 1144 (1975).

[2]P. R. Berman and W. E. Lamb, Jr., Phys. Rev. A 2, 2435 (1970); 4, 319 (1971); E. W. Smith, J. Cooper, W. R. Chappell, and T. Dillon, J. Quant. Spectrosc. Radiat. Transfer 11, 1547, 1567 (1971); W. R. Chappell, J. Cooper, E. W. Smith, and T. Dillon, J. Stat. Phys. 3, 401 (1971); V. A. Alexseev, T. L. Andreeva, and I. I. Sobelman, Zh. Eksp. Teor. Fiz. 62, 614 (1972) [Sov. Phys.—JETP 35, 325 (1972)]; 64, 813 (1973) [37, 413 (1973)]. For additional references, see the review article by P. R. Berman, Appl. Phys. (Germany) 6, 283 (1975).

[3]P. R. Berman, Phys. Rev. A 5, 927 (1972).

[4]P. R. Berman, Phys. Rev. A 6, 2157 (1972).

[5]*Laser Spectroscopy*, edited by R. G. Brewer and A. Mooradian (Plenum, New York, 1974).

[6]T. W. Hänsch and P. E. Toschek, IEEE J. Quantum Electron. QE-5, 61 (1969).

[7]P. W. Smith and T. W. Hänsch, Phys. Rev. Lett. 26, 740 (1971).

[8]R. Keil, A. Schabert, and P. Toschek, Z. Phys. 261, 71 (1973).

[9]I. M. Beterov, Y. A. Matyugin, and V. P. Chebotaev, Zh. Eksp. Teor. Fiz. 64, 1495 (1973) [Sov. Phys.—JETP 37, 756 (1973)].

[10]W. K. Bischel, P. J. Kelley, and C. K. Rhodes, Phys. Rev. Lett. 34, 300 (1975).

[11]D. L. Rousseau, G. D. Patterson, and P. F. Williams, Phys. Rev. Lett. 34, 1306 (1975).

[12]D. E. Roberts and E. N. Fortson, Phys. Rev. Lett. 31, 1593 (1973); D. Pritchard, J. Apt, and T. W. Ducas, *ibid.* 32, 641 (1974); F. Biraben, B. Cagnac, and G. Grynberg, *ibid.* 32, 643 (1974); M. D. Levenson and N. Bloembergen, *ibid.* 32, 645 (1974); T. W. Hänsch, K. C. Harvey, G. Meisel, and A. L. Schawlow, Opt. Commun. 11, 50 (1974).

[13]P. F. Liao and J. E. Bjorkholm, Phys. Rev. Lett. 33, 128 (1974).

[14]S. G. Rautian and A. A. Feoktistov, Zh. Eksp. Teor. Fiz. 56, 227 (1969) [Sov. Phys.—JETP 29, 126 (1969)].

[15]T. W. Hänsch and P. E. Toschek, Z. Phys. 236, 213 (1970).

[16]S. G. Rautian, G. I. Smirnov, and A. M. Shalagin, Zh. Eksp. Teor. Fiz. 62, 2097 (1972) [Sov. Phys.—JETP 35, 1095 (1972)].

[17]A. P. Kolchenko, A. A. Pukhov, S. G. Rautian, and A. M. Shalagin, Zh. Eksp. Teor. Fiz. 63, 1173 (1972) [Sov. Phys.—JETP 36, 619 (1973)].

[18]W. Heitler, *The Quantum Theory of Radiation*, 3rd ed. (Oxford U.P., Oxford, 1954), Sec. V-20.

[19]Y. R. Shen, Phys. Rev. B 9, 622 (1974).

[20]R. G. Brewer and E. L. Hahn, Phys. Rev. A 11, 1641 (1975).

[21]The amplitude of fluorescence at a given angle to the incident laser beam will, in general, depend on specific density matrix elements $\rho_{3m;3m'}$.

[22]A. Omont, E. W. Smith, and J. Cooper, Astrophys. J. 175, 185 (1972).

[23]If both γ_1 and γ_3 approach zero, a steady-state solution of Eqs. (16) is no longer possible. Instead, $I_{mm'} \propto t$.

[24]The propogator bears some resemblance to the collision kernel proposed by J. Keilson and J. E. Storer, Q. Appl. Math. 10, 243 (1952). Equation (44) represents an approximate solution to Eq. (40) for that propagator—an exact solution is easy to obtain but would involve an infinite summation.

[25]The contour integrals are performed more easily on Eq. (36a) than Eq. (41a).

[26]U. Fano and G. Racah, *Irreducible Tensorial Sets* (Academic, New York, 1962); A. Ben-Reuven, Phys. Rev. 141, 34 (1966); 145, 7 (1966).

[27]As an example of a more realistic form for $P_{-11}(\alpha)$, one could take the solution of Eqs. (35), neglecting velocity-changing collisions and assuming isotropic collisions by perturber atoms. Berman and Lamb performed a related calculation [P. R. Berman and W. E. Lamb, Jr., Phys. Rev. 187, 221 (1969)] from which one would deduce

$$P_{-11} = [\gamma_2 T_2 + T_1(T_1 + 2T_2)]/[(\gamma_2 + T_1 + 2T_2)\gamma_2(\gamma_2 + 3T_1)],$$

where T_1 is the collisional rate of transfer from $m = 0$ to $m = 1$ and T_2 the rate of transfer from $m = -1$ to $m = 1$. For a Van der Waals interaction, $T_1/T_2 = 0.847$.

[28]R. H. Dicke, Phys. Rev. 103, 620 (1956).

[29]A calculation of resonant excitation transfer, taking into account the quantum-mechanical aspects of collisions, has been given by H. R. Zaidi, Can. J. Phys. 50, 2801 (1972).

[30]Off-diagonal elements can be transferred only if level 1 is a thermally populated ground state.

[31]M. I. D'Yakonov and V. F. Perel, Zh. Eksp. Teor. Fiz. 47, 1483 (1964) [Sov. Phys.—JETP 20, 997 (1965)]; A. Omont, J. Phys. (Paris) 26, 576 (1965); M. I. D'Yakonov and V. I. Perel, Zh. Eksp. Teor. Fiz. 58, 1090 (1970) [Sov. Phys.—JETP 31, 585 (1970)]; I. M. Beterov, Y. A. Matyugin, S. G. Rautian, and V. P. Chebotaev, *ibid.* 58, 1243 (1970) [31, 668 (1970)]; V. I. Perel and I. V. Rogova, *ibid.* 61, 1814 (1971) [34, 965 (1972)].

[32]If level 1 is a ground state, the situation is more complex. Calculations exist [e.g., H. R. Zaidi, Phys. Rev. 173, 123 (1968)] which claim that off-diagonal

elements can be transferred or, at the very least, altered by radiation trapping. Such effects would be most important in the TQ chain, and additional studies of radiation trapping could help clarify this point.

[33]M. S. Feld and A. Javan, Phys. Rev. 177, 540 (1969); E. V. Baklonov and V. P. Chebotaev, Zh. Eksp. Teor. Fiz. 60, 552 (1971) [Sov. Phys.—JETP 33, 300 (1971)]; S. Haroche and F. Hartmann, Phys. Rev. A 6, 1280 (1972); R. Salomaa and S. Stenholm, J. Phys. B 8, 1795 (1975).

[34]T. W. Meyer and C. K. Rhodes, Phys. Rev. Lett. 32, 637 (1974).

[35]R. G. Brewer, R. L. Shoemaker, and S. Stenholm, Phys. Rev. Lett. 33, 63 (1974); R. L. Shoemaker, S. Stenholm, and R. G. Brewer, Phys. Rev. A 10, 2037 (1974).

[36]J. Schmidt, P. R. Berman, and R. G. Brewer, Phys. Rev. Lett. 31, 1103 (1973); P. R. Berman, J. M. Levy, and R. G. Brewer, Phys. Rev. A 11, 1668 (1975).

[37]In recent saturated absorption experiments on Xe, there is some evidence of large velocity changes produced in Xe-Xe collisions (private communication from R. Vetter).

[38]Equations (A7) and (A8) correct an error made in Eqs. (19)–(21) of Ref. 4.